ADVANCED FFAG OPTICS, DESIGN AND EXPERIMENT

JB. Lagrange, Y. Mori,

KURRI, Osaka, Japan

Motivation

- Strong revival of FFAGs in the last decade, but still big limitations in lattice design:
  - Circular machine only.
  - limited drift space for cavities, injection and extraction.
  - too large excursion for very high frequency acceleration.
  - one type of cell per machine $\rightarrow$ no insertion.

Motivation

- Strong revival of FFAGs in the last decade, but still big limitations in lattice design:
  - Circular machine only.
  - limited drift space for cavities, injection and extraction.
  - too large excursion for very high frequency acceleration.
  - one type of cell per machine → no insertion.

→ **Needs for innovative transverse focusing in zero-chromatic systems.**

Outline

Outline

- Classic case: horizontal excursion circular FFAG

Outline

- Classic case: horizontal excursion circular FFAG
- Straight zero-chromatic FFAG

Outline

- Classic case: horizontal excursion circular FFAG
- Straight zero-chromatic FFAG
- FFAG insertions

Outline

- Classic case: horizontal excursion circular FFAG
- Straight zero-chromatic FFAG
- FFAG insertions
- Vertical excursion FFAG

Outline

- Classic case: horizontal excursion circular FFAG
- Straight zero-chromatic FFAG
- FFAG insertions
- Vertical excursion FFAG
- Fixed frequency acceleration in zero-chromatic FFAGs

Outline

- Classic case: horizontal excursion circular FFAG
- Straight zero-chromatic FFAG
- FFAG insertions
- Vertical excursion FFAG
- Fixed frequency acceleration in zero-chromatic FFAGs

Invariance of the betatron oscillations

keep independent of momentum the transverse linearized equations of motion.

➡ zero-chromatic system for any momentum range.

Circular case

Linearized equations of motion for a momentum p:

$$\begin{cases} \dfrac{d^2x}{d\Theta^2} + \dfrac{R^2}{\rho^2}(1-n)x = 0, \\ \dfrac{d^2z}{d\Theta^2} + \dfrac{R^2}{\rho^2}nz = 0. \end{cases}$$

(x, s, z): curvilinear coordinates.

New system of coordinates (x, Θ, z)

$\Theta = s/R$ with $R = \dfrac{1}{2\pi}\oint ds$

n: field index

ρ : curvature radius

Independent of momentum p:

$$\begin{cases} \left(\dfrac{\partial(R/\rho)}{\partial p}\right)_\Theta = 0, \\ \left(\dfrac{\partial n}{\partial p}\right)_\Theta = 0. \end{cases}$$

$\Rightarrow$ Similarity of the reference trajectories.

$\Rightarrow$ Invariance of the focusing strength.

Circular case

Invariance of the betatron oscillations $\Longleftrightarrow$ similarity of the closed orbits <u>and</u> invariance of the field index

Geometrical field index: $k = \frac{R}{\bar{B}}\frac{d\bar{B}}{dR}$

$$\boxed{B(r,\theta) = B_0\left(\frac{r}{r_0}\right)^k \cdot \mathcal{F}(\theta - \tan\zeta \ln \frac{r}{r_0})}$$

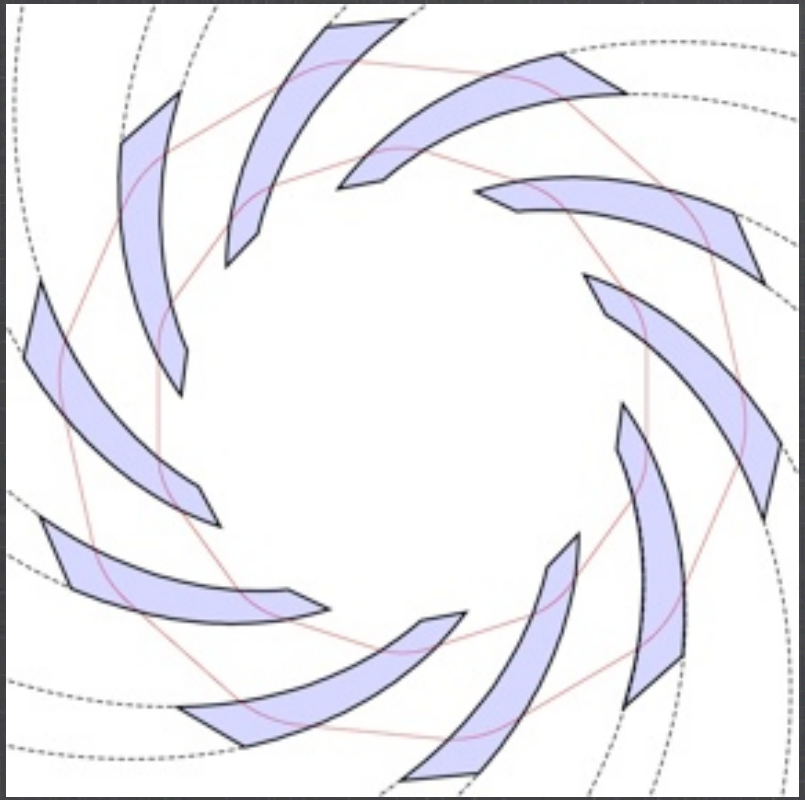

Spiral sector: $\zeta = const.$

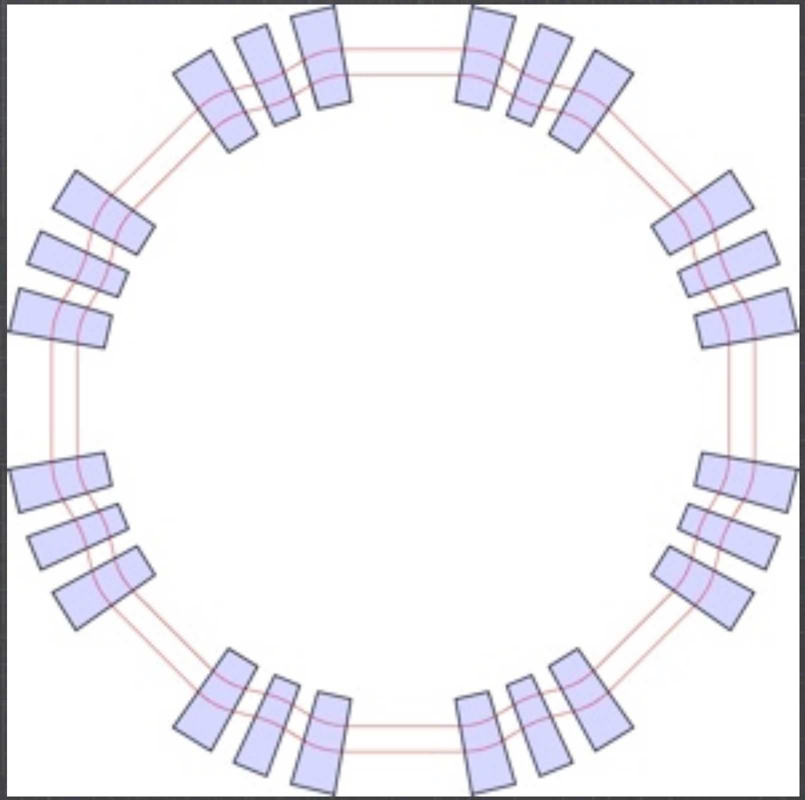

Radial sector: $\zeta = 0$

Outline

- Classic case: horizontal excursion circular FFAG
- Straight zero-chromatic FFAG
  - Theory
  - Experiment
- FFAG insertions
- Vertical excursion FFAG
- Fixed frequency acceleration in zero-chromatic FFAGs

New case: straight case

Linearized equations of motion for a momentum *p*:

$$\begin{cases} \dfrac{d^2x}{ds^2} + \dfrac{1-n}{\rho^2}x = 0, \\ \dfrac{d^2z}{ds^2} + \dfrac{n}{\rho^2}z = 0. \end{cases}$$

(x, s, z): curvilinear coordinates

n: field index

ρ : curvature radius

Independent of momentum *p:*

$$\begin{cases} \left(\dfrac{\partial \rho}{\partial p}\right)_s = 0, \\ \left(\dfrac{\partial n}{\partial p}\right)_s = 0. \end{cases}$$

$\left(\dfrac{\partial \rho}{\partial p}\right)_s = 0 \Rightarrow$ Similarity of the reference trajectories

$\left(\dfrac{\partial n}{\partial p}\right)_s = 0 \Rightarrow$ Invariance of the focusing strength

Change of coordinates: introduction of average abscissa χ.

New case: straight case

Introduction of normalized field gradient: $m = \frac{1}{B}\frac{dB}{d\chi}$

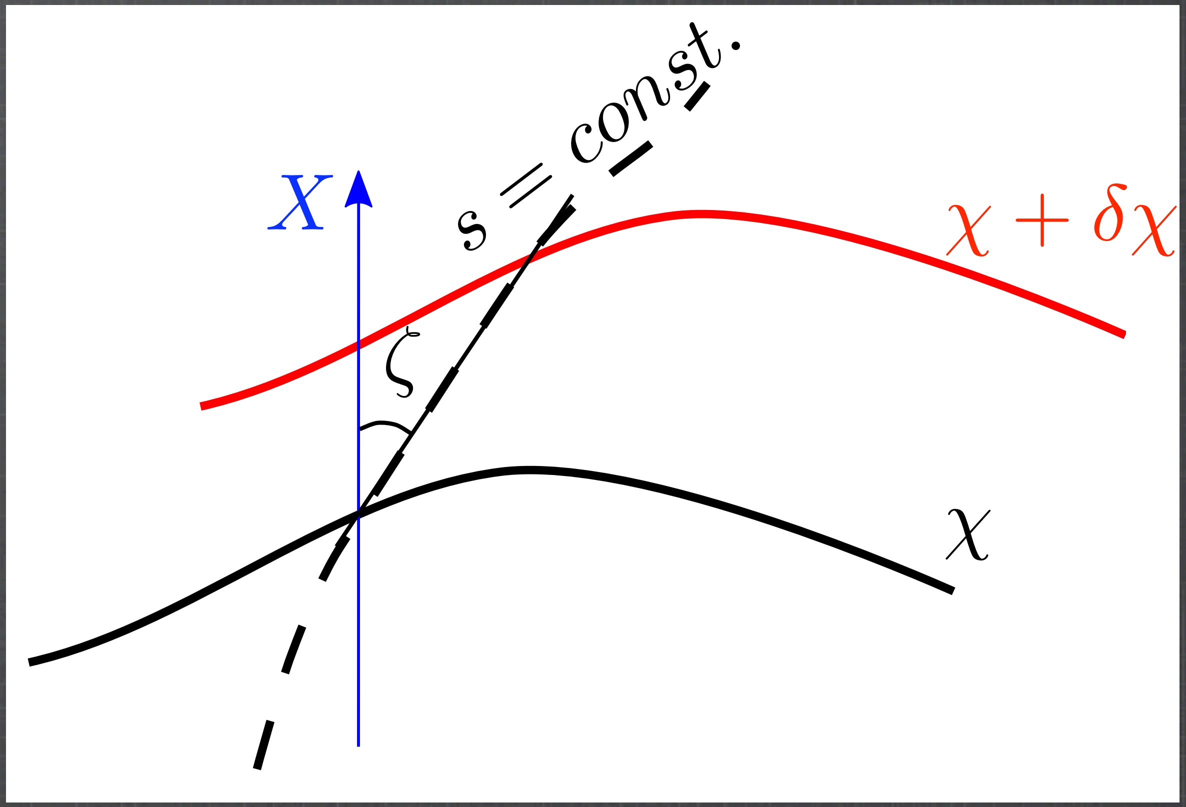

Invariance of the focusing strength gives condition on *m:*

$$m = m_1 + m_2 \tan\zeta(\chi)$$

$$\boxed{B(\chi, s) = B_0 e^{\left[m_1(\chi - \chi_0) + m_2 \int_{\chi_0}^{\chi} \tan\zeta(\chi) d\chi\right]} \mathcal{F}(s)}$$

New case: straight case

$\zeta = const. \Longleftrightarrow m = const.$

$$\boxed{B(X,Y) = B_0 e^{m(X-X_0)} \mathcal{F}\left(Y - (X - X_0)\tan\zeta\right)}$$

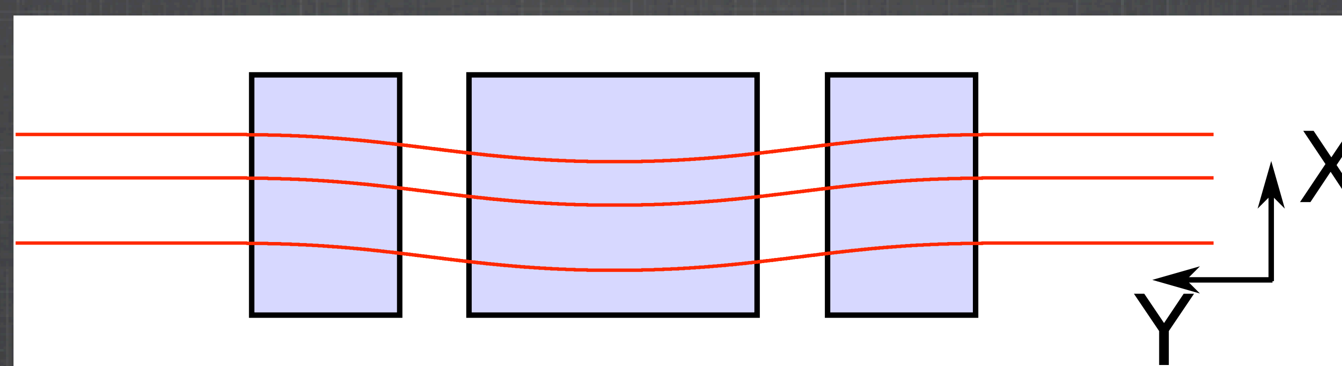

Rectangular case: $\zeta = 0$

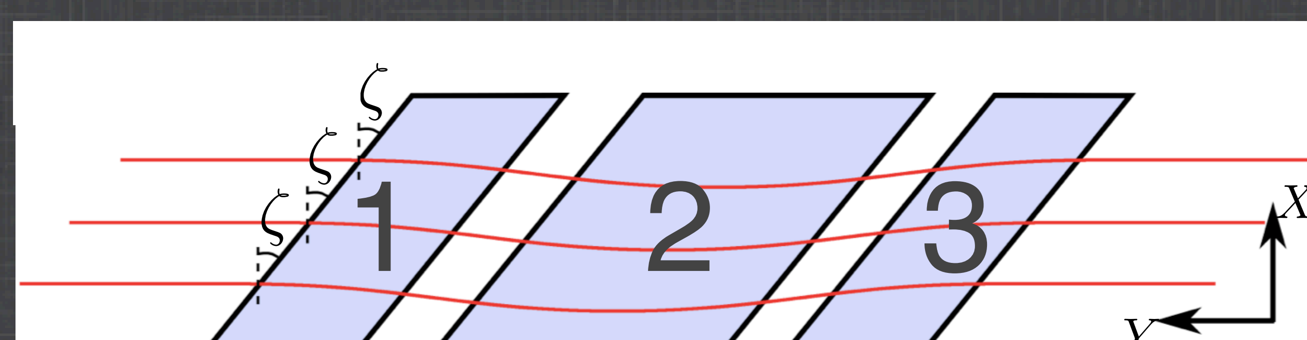

Tilted straight case: $\zeta = const.$

Straight scaling FFAG experiment

Design and manufacturing of a straight scaling cell prototype, and measure of the horizontal phase advance for 2 different energies.

Layout of the experiment

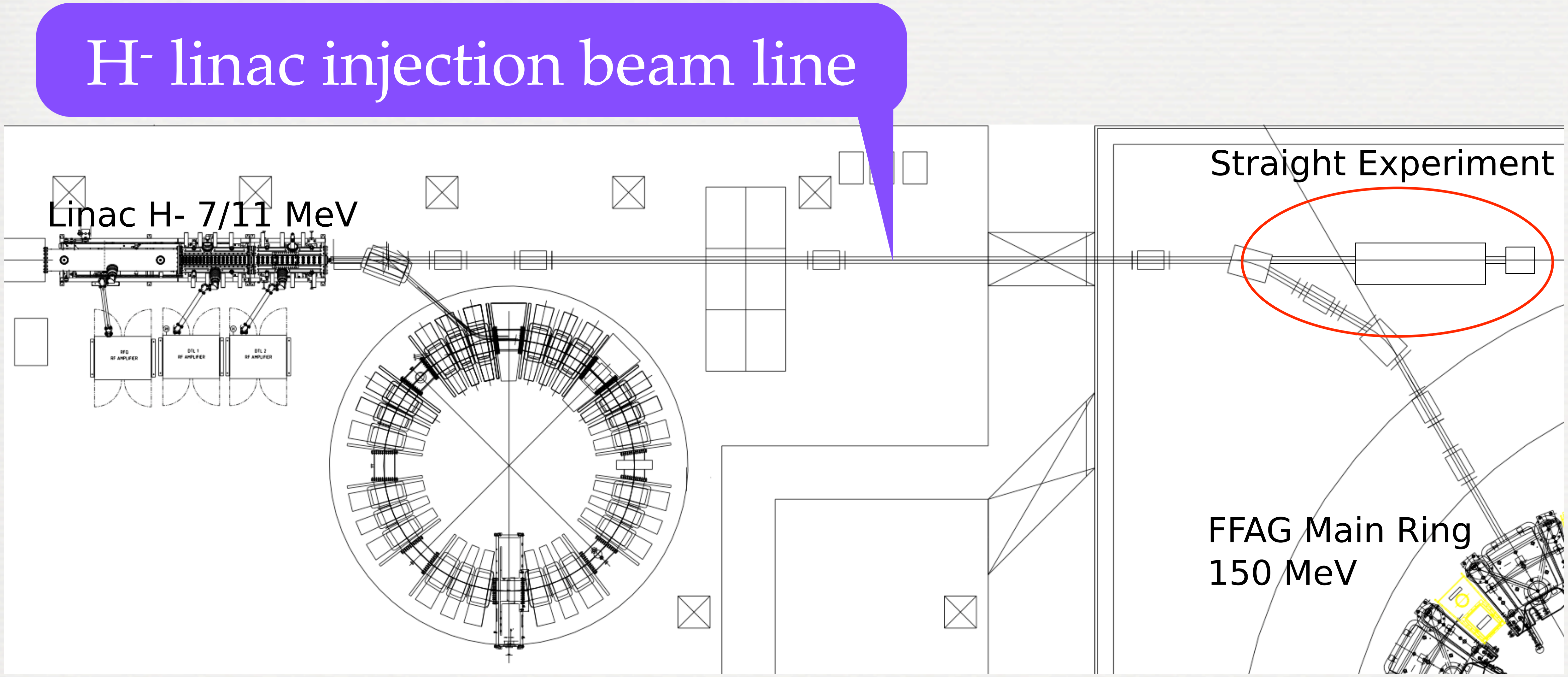

Use of 2 energies: 7 MeV and 11 MeV.

Layout of the experiment

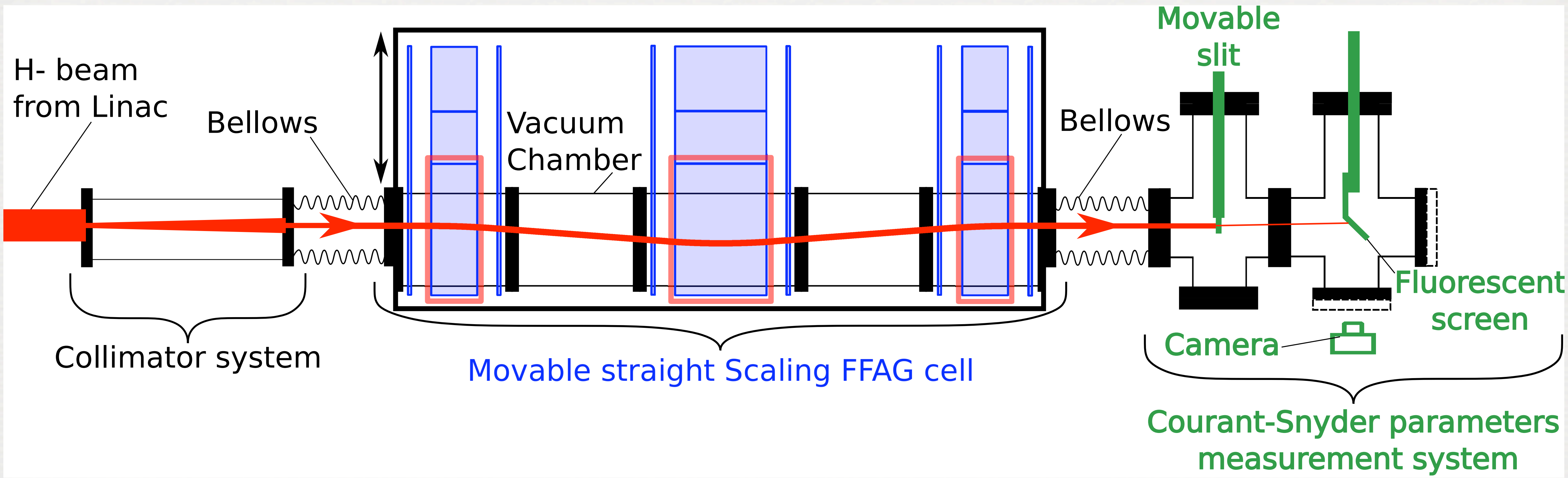

Layout of the experiment

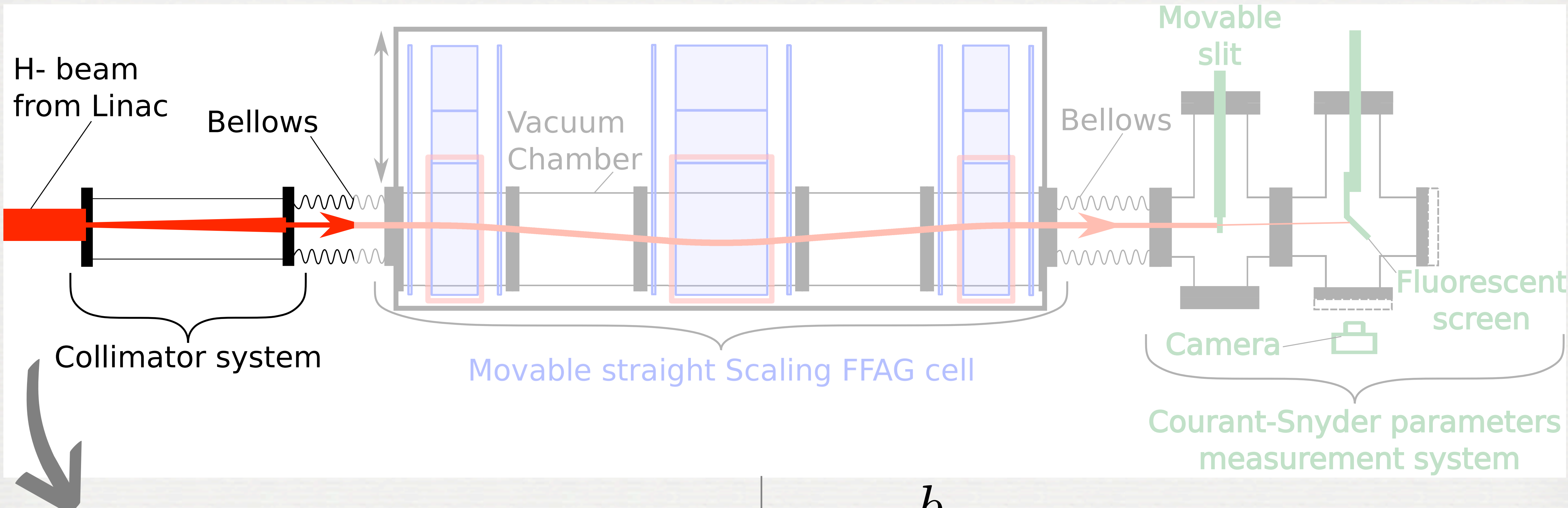

Set the entrance linear parameters (β_0 and α_0) and emittance (ε).

$$\beta_0 = \frac{b}{2} = 0.77\ m$$

$$\alpha_0 = 0$$

$$\epsilon_{rms} = \frac{a^2}{18b} = 0.14\ \pi\ mm.mrad$$

Layout of the experiment

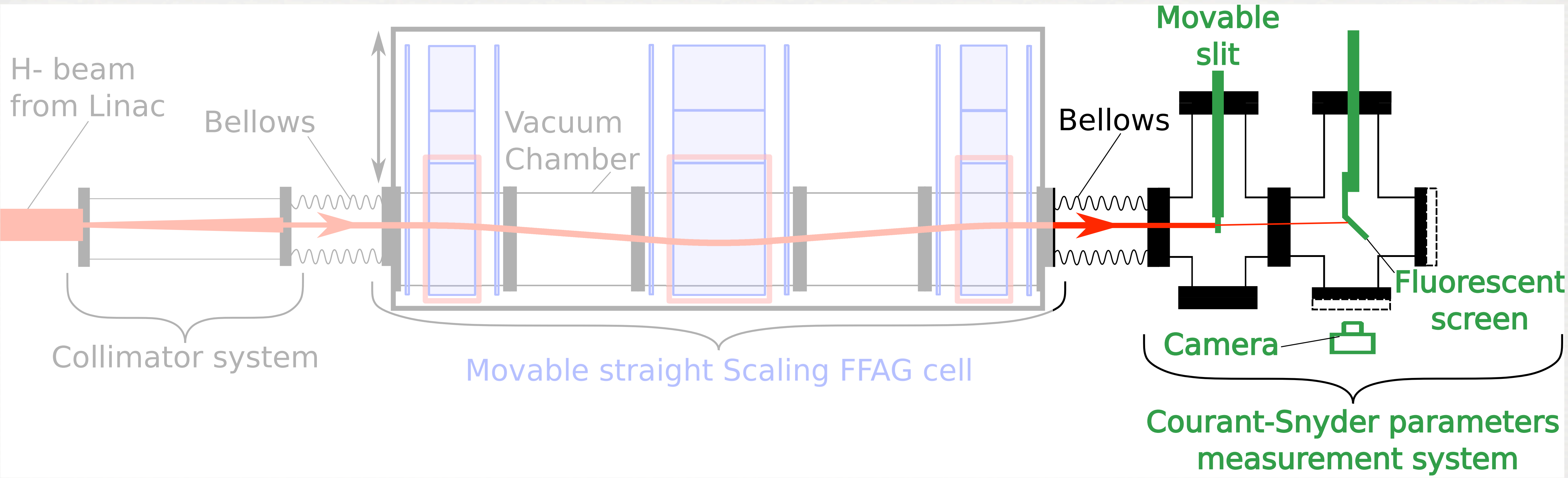

Measure linear parameters (β_1 and α_1), position and angle of the beam.

Layout of the experiment

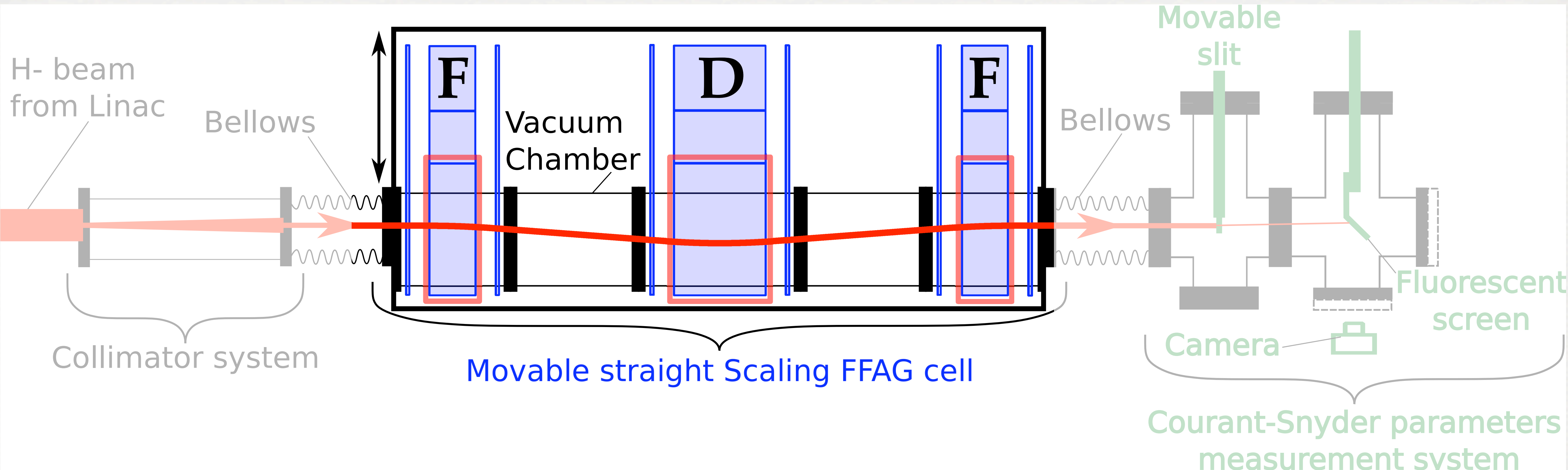

Straight Scaling FFAG cell design

- C-shape Magnets to have easy access to the pole.
- Cell able to move horizontally to match the different reference trajectories.
- Rectangular magnets.

Type	FDF
m-value	11 m^{-1}
Total length	4.68 m
Length of F magnet	15 cm
Length of D magnet	30 cm
Max. B Field (D magnet)	0.3 T
Max. B Field (F magnet)	0.2 T
Horizontal phase advance	87.7 deg.
Vertical phase advance	106.2 deg.

- Coils:
  - Max 3500 A.T/coil.
  - 18 turns x 4 layers = 72 turns of 5 mm x 2 mm cross section wire.

→ ~5 A/mm² → Indirect water cooling system.

- Power supply per magnet (D): 100 A, 30 V.
- Whole system power consumption: ~1 kW.

Magnet design

Pole shape configured with POISSON, then TOSCA.

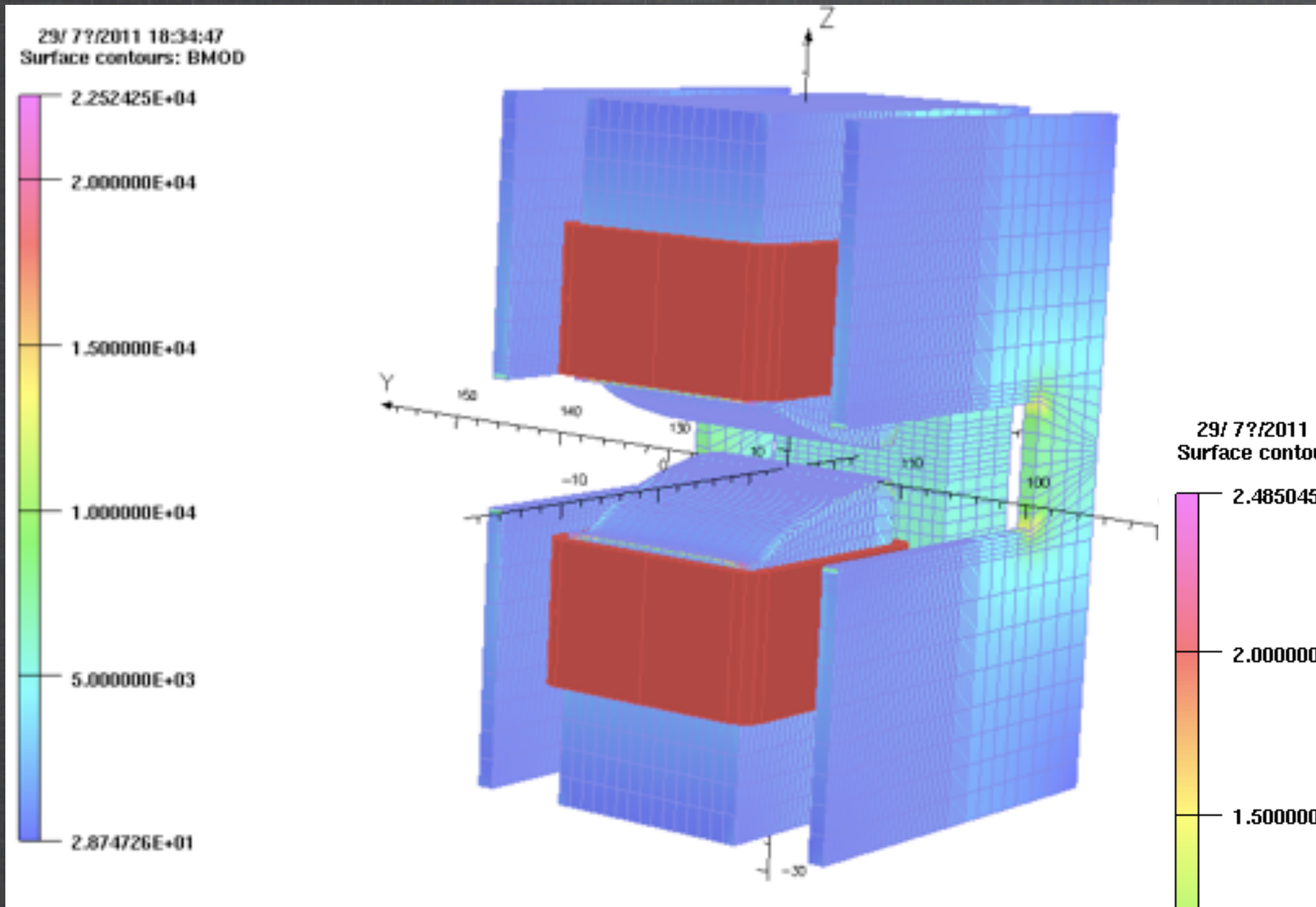

Magnetic field in D magnet (30 cm long). TOSCA model.

Magnetic field in F magnet (15 cm long). TOSCA model.

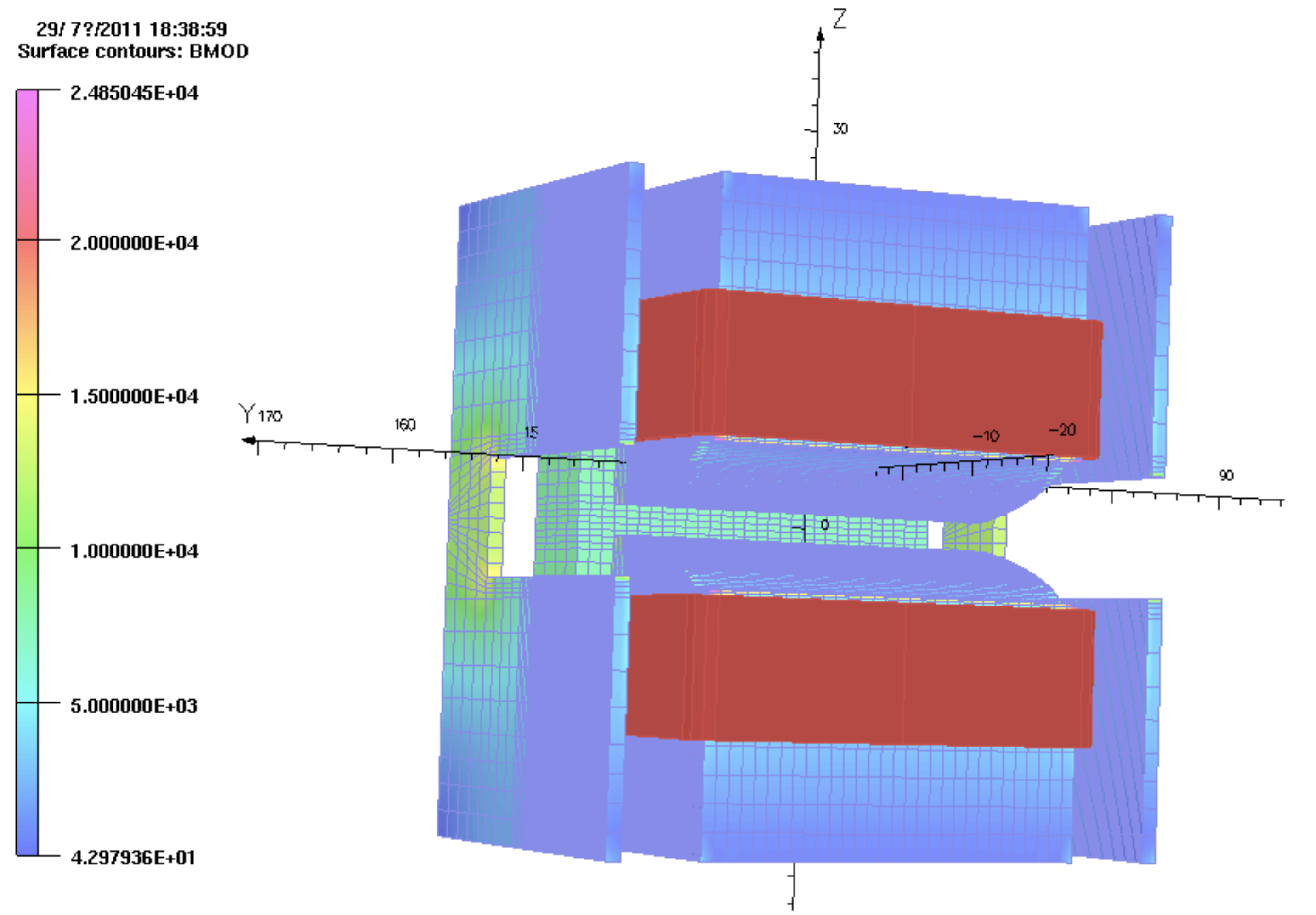

Field in TOSCA Field map

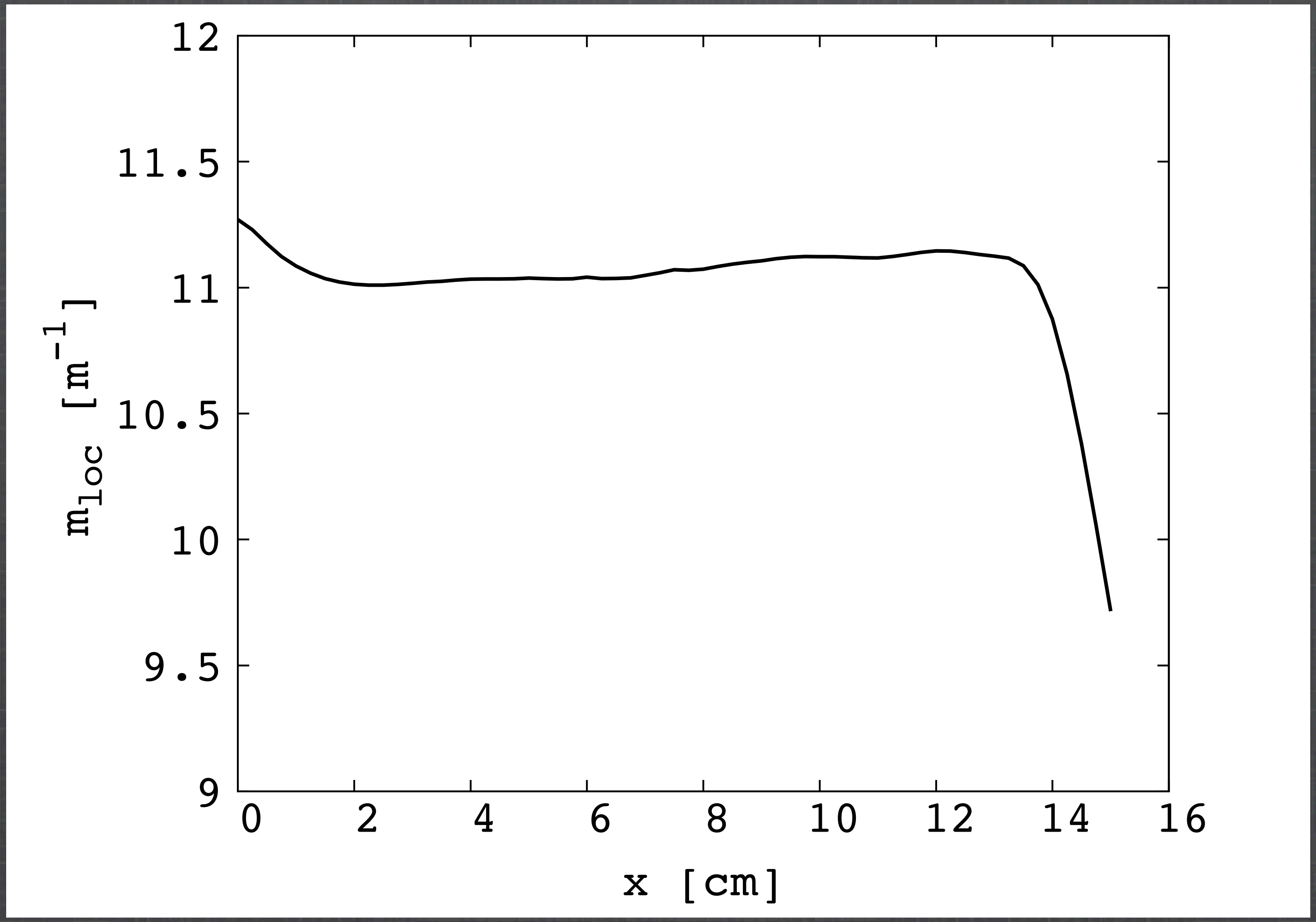

Local m value vs horizontal abscissa

$$\begin{cases} m(X_i) = \ln\left[\frac{\int B_z(X_i,Y)dY}{\int B_z(X_{ref},Y)dY}\right] \cdot \frac{1}{X_i - X_{ref}}, \\ m(X_{ref}) = \frac{m(X_{ref-1}) + m(X_{ref+1})}{2}. \end{cases}$$

FIELD MEASUREMENT

Measured field map created

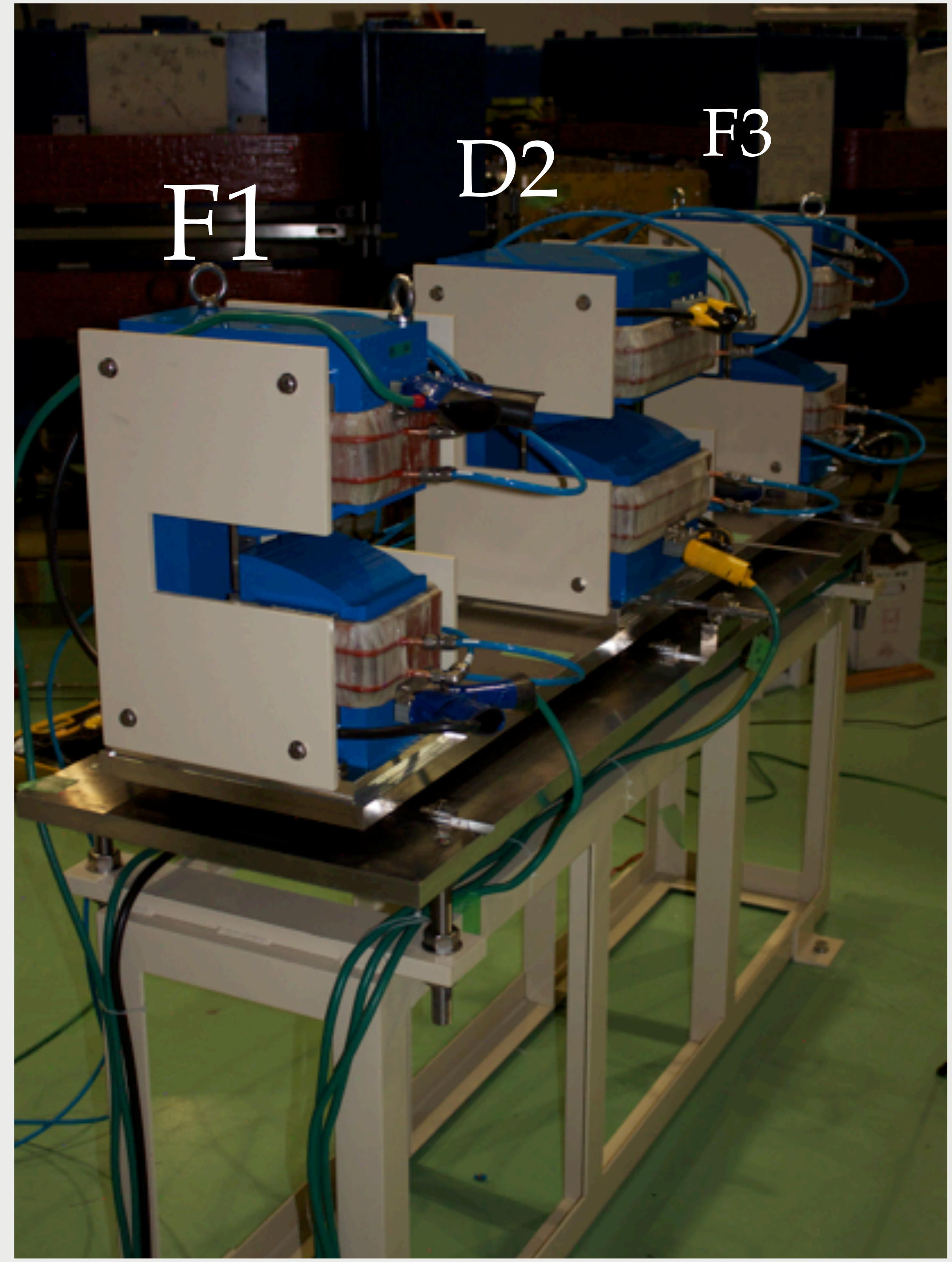

Comparison TOSCA-Measure

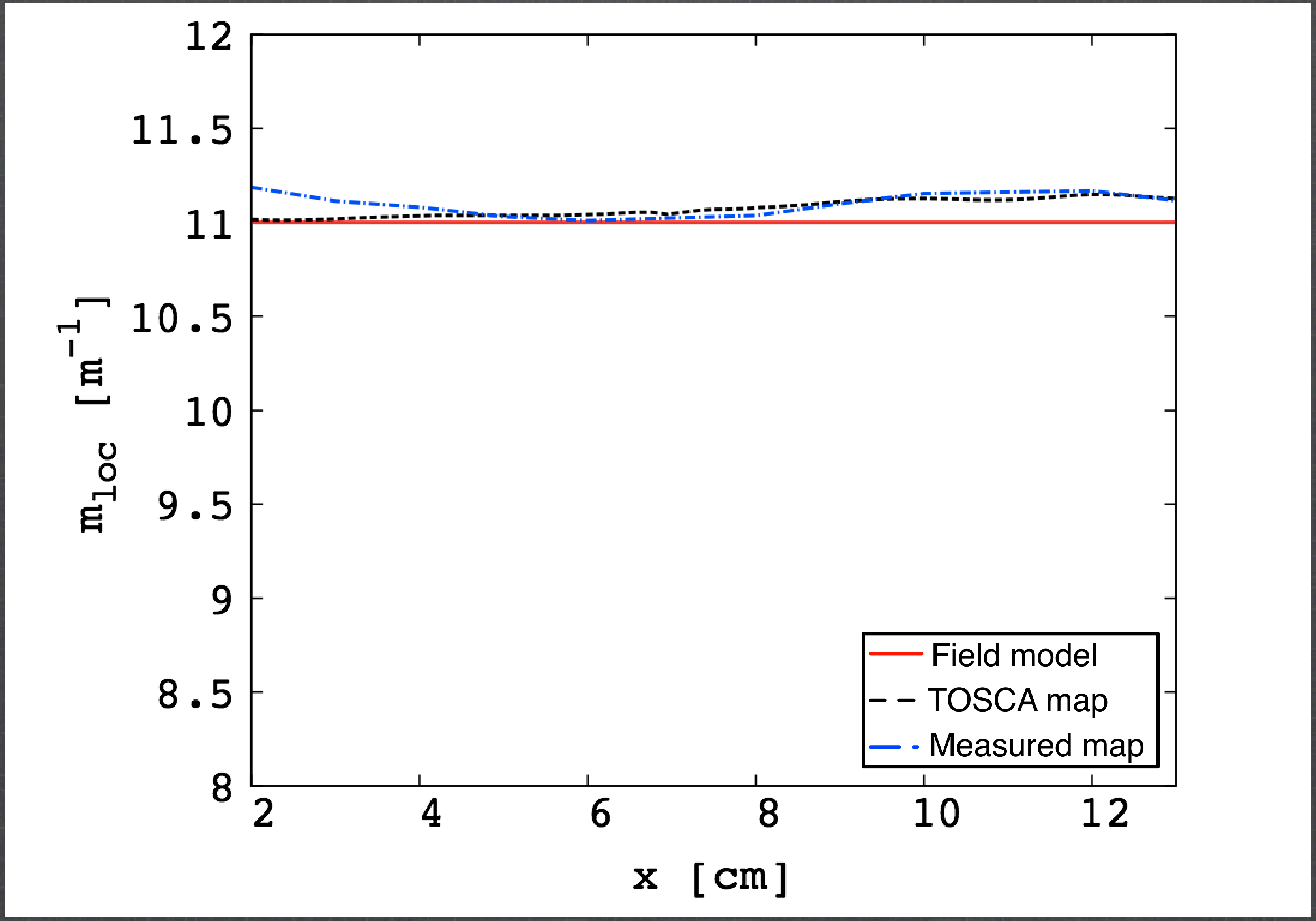

Local m-value vs horizontal abscissa with field model (plain red), in TOSCA field map (black dashed) and in measured field map (mixed blue).

→ **<u>Good agreement</u>** (difference < 1%)

Particle tracking

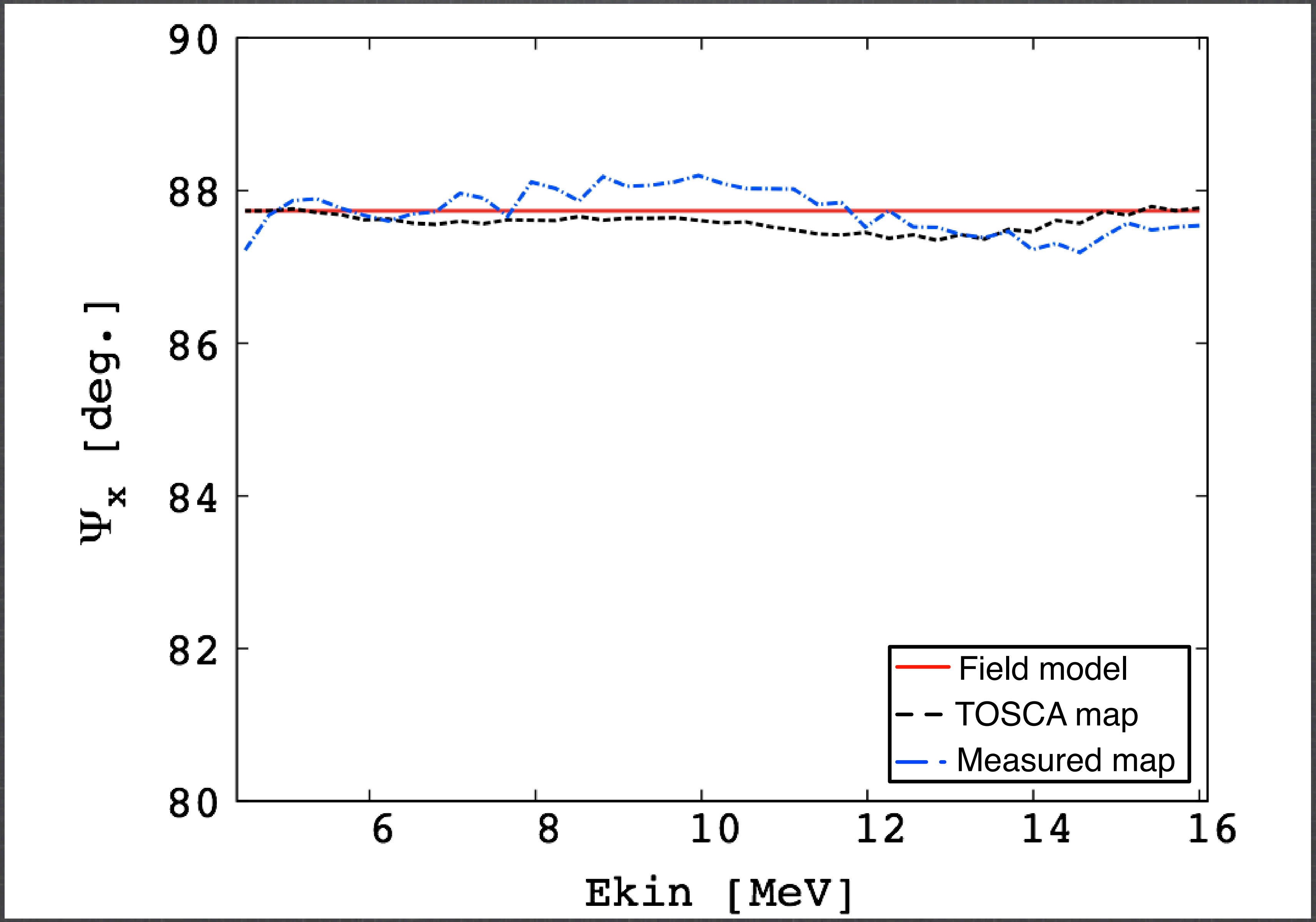

Horizontal phase advances vs kinetic energy with field model (plain red), in TOSCA field map (black dashed) and in measured field map (mixed blue).

Experimental measurement

$$\begin{pmatrix} x_1 \\ x'_1 \end{pmatrix} = \begin{pmatrix} \sqrt{\frac{\beta_1}{\beta_0}} \cos\psi & a_{12} \\ \frac{-\alpha_1 \cos\psi - \sin\psi}{\sqrt{\beta_1 \beta_0}} & a_{22} \end{pmatrix} \cdot \begin{pmatrix} x_0 \\ 0 \end{pmatrix}$$

$$\Rightarrow \tan\psi = -\alpha_1 - \frac{\beta_1 x'_1}{x_1}$$

Exit parameters to measure: x_1, x'_1, β_1 and α_1.

For each energy, the beam is launched 3 times:

- on the reference trajectory,
- -10 mm off the reference trajectory,
- +10 mm off the reference trajectory.

$$\Rightarrow \boxed{\begin{aligned} x_1 &= \frac{x_{+10} - x_{-10}}{2} \\ x'_1 &= \frac{x'_{+10} - x'_{-10}}{2} \end{aligned}}$$

Experimental measurement

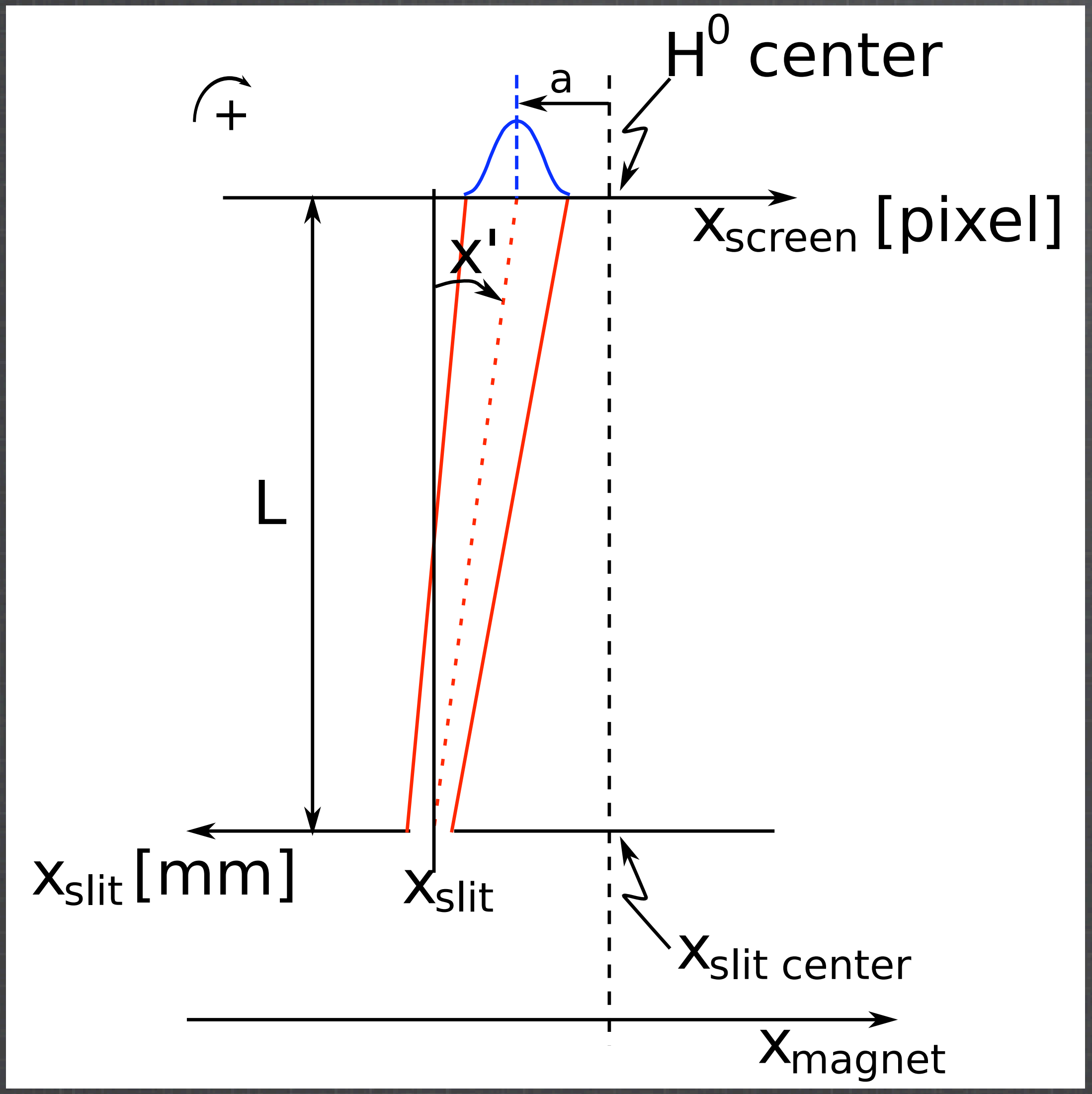

angle measurement scheme.

position and beta measurement from pictures without slit.

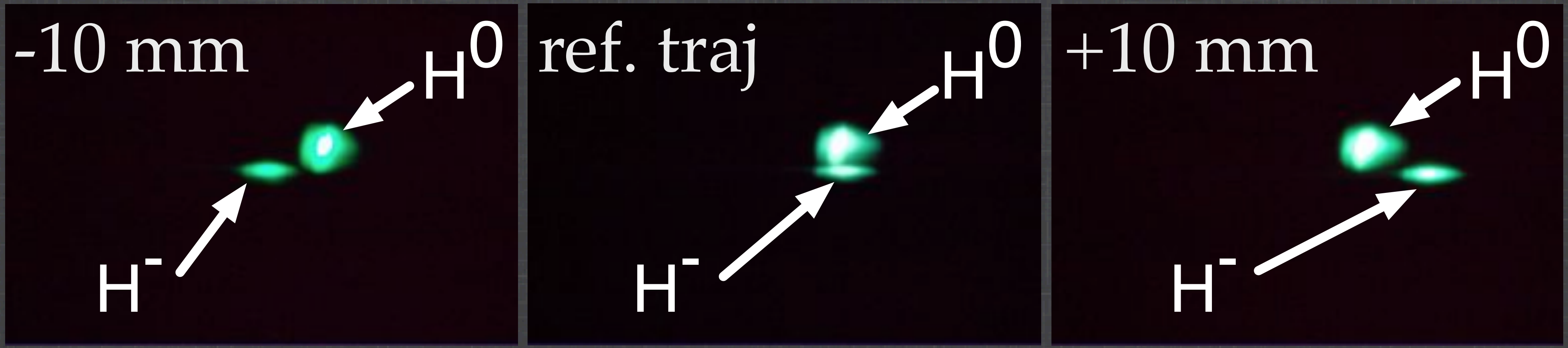

Experimental measurement

α_1 measurement from

- the slope of the line x' vs. x_{slit}: $slope = -\left(\frac{\alpha}{\beta}\right)_{slit}$
- the beta value

→ Drift transfer matrix tracking to obtain α_1.

Experimental results

$$\tan\psi = -\alpha_1 - \frac{\beta_1 x_1'}{x_1}$$

	$\bar{x_1}$ (mm)	$\bar{x_1'}$ (mrad)	$\bar{\beta_1}$ (m)	$\bar{\alpha_1}$	$\psi_{exp.}$ (deg)	ψ_{TOSCA} (deg)
11 MeV	**2.0**	**-2.4**	**17.7**	**-1.5**	**87.5** $\pm$ 3.3	**87.5**
7 MeV	**1.8**	**-2.1**	**11.7**	**-1.0**	**86.1** $\pm$ 9.6	**87.6**

ψ_{exp}(11 MeV)=87.5 deg

ψ_{exp}(7 MeV)=86.1 deg

Straight scaling law clarified.

J.-B. Lagrange *et al*, "Straight scaling FFAG beam line",
Nucl. Instr. Meth. A, vol. 691, pp. 55–63, 2012.

Outline

- Classic case: horizontal excursion circular FFAG
- Straight zero-chromatic FFAG
- FFAG insertions
  - Combination of scaling FFAG cells
  - Dispersion suppressor
- Vertical excursion FFAG
- Fixed frequency acceleration in zero-chromatic FFAGs

FFAG insertions

Matching of different scaling FFAG cells

1) Matching of the curves s = const.

Radial for the circular case, rectangular in the straight case.

2) Matching of the reference trajectories

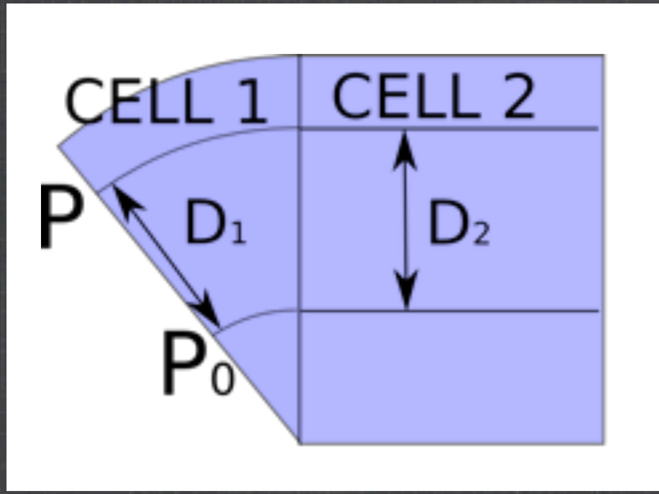

a) Matching of a special momentum P_0.

b) Matching to the first order in $\Delta R/R_0$ by matching of the cell dispersion of the different parts.

3) Matching of the periodic linear parameters

Often difficult → π-phase advance for one of the parts

Insertions

Matching of different scaling FFAG cells

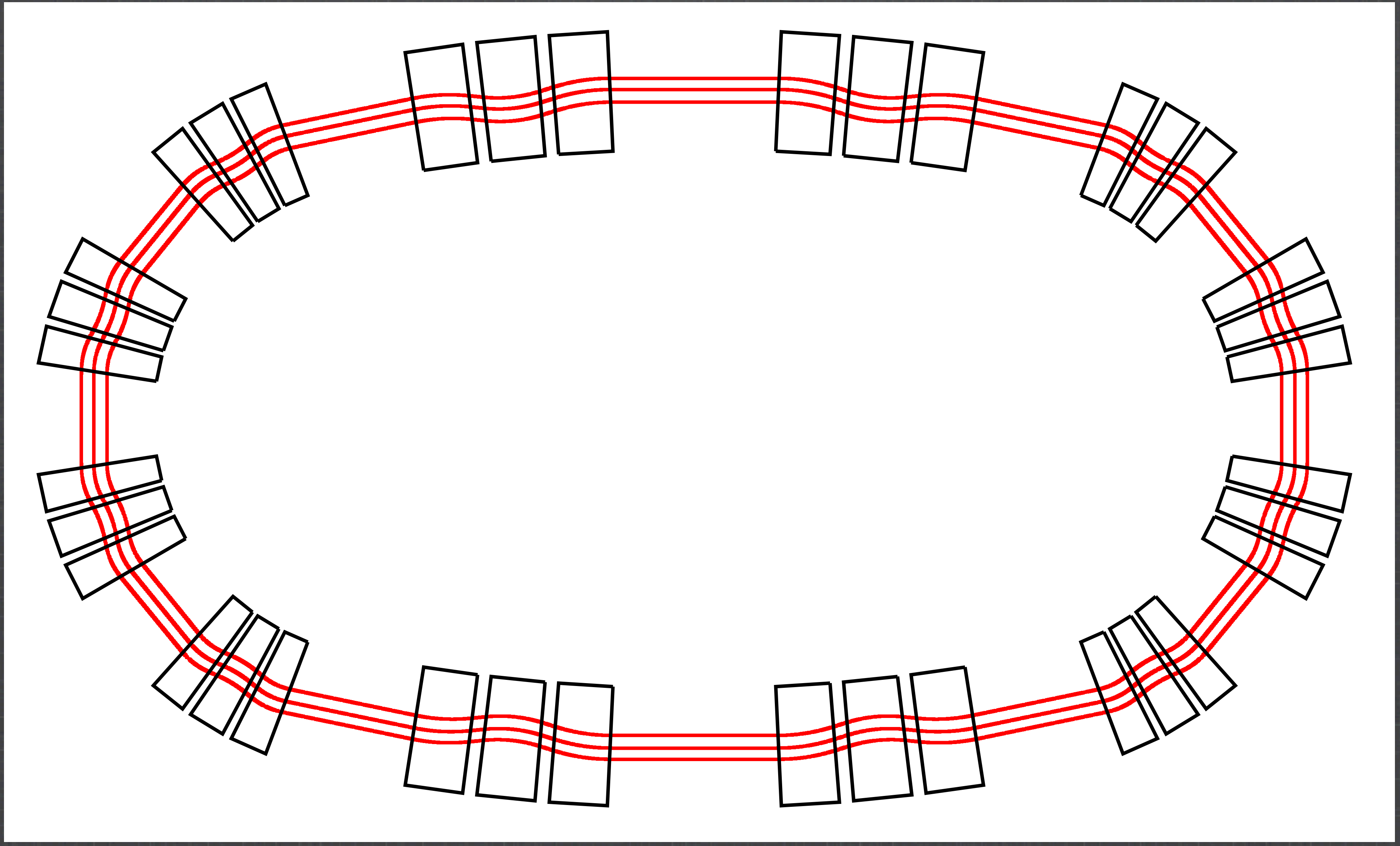

Insertions

Matching of different scaling FFAG cells

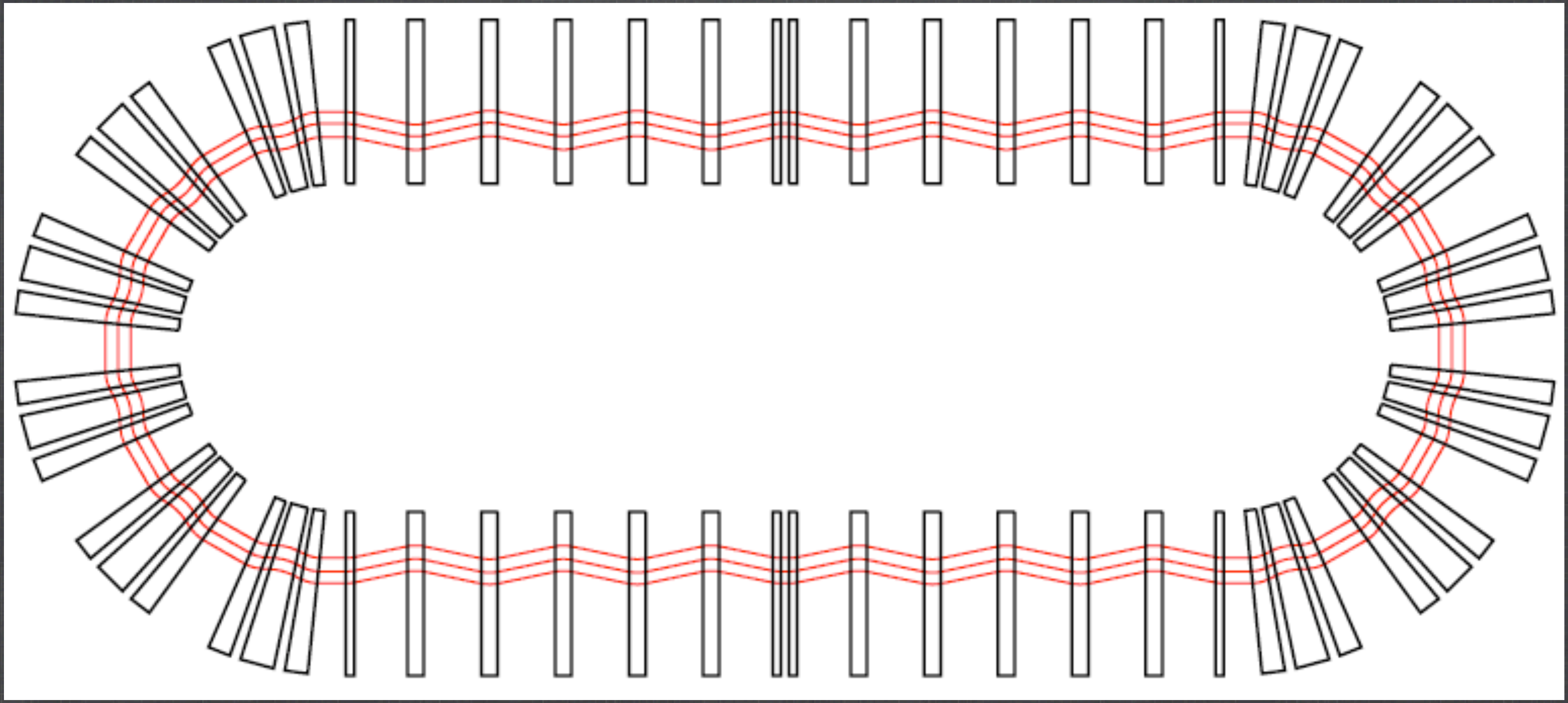

Application: nuSTORM

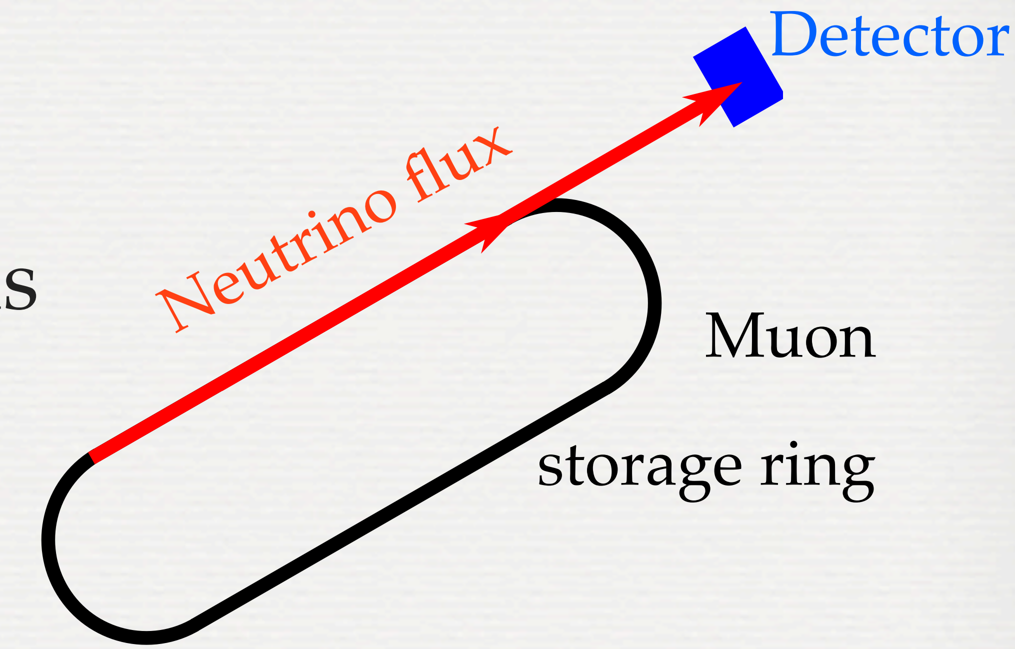

<u>**Neutrinos from STORed Muons**</u> (nuSTORM) with a muon storage ring is investigated for neutrino experiments (neutrino mixing matrix).

Muons decay in neutrinos in the storage ring

→ <u>Racetrack</u> to collect the maximum decayed neutrinos.

Conventional racetrack storage ring has small longitudinal acceptance: $\frac{\Delta p}{p} \sim \pm 1\%$

Dramatically reduces the brightness at the detector.

→ <u>Racetrack FFAG</u> design

Applications: nuSTORM

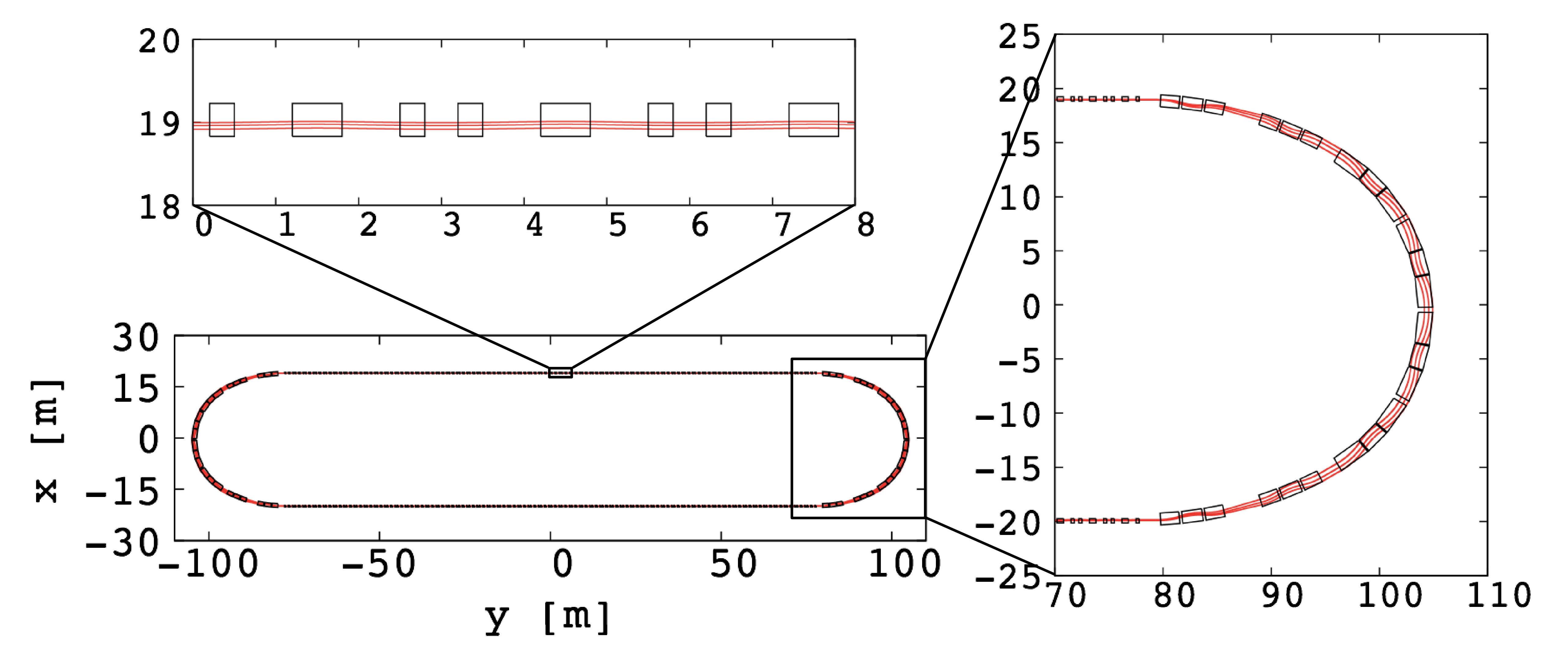

Large transverse acceptance (1000π mm.mrad)

Large momentum acceptance (±16%, up to ±25%)

Insertions

Dispersion suppressor principle

Use of 3 different scaling FFAG cells

a) Matching of a special momentum P_0.

b) Matching of cell dispersions such as $D_2 = \dfrac{D_1 + D_3}{2}$

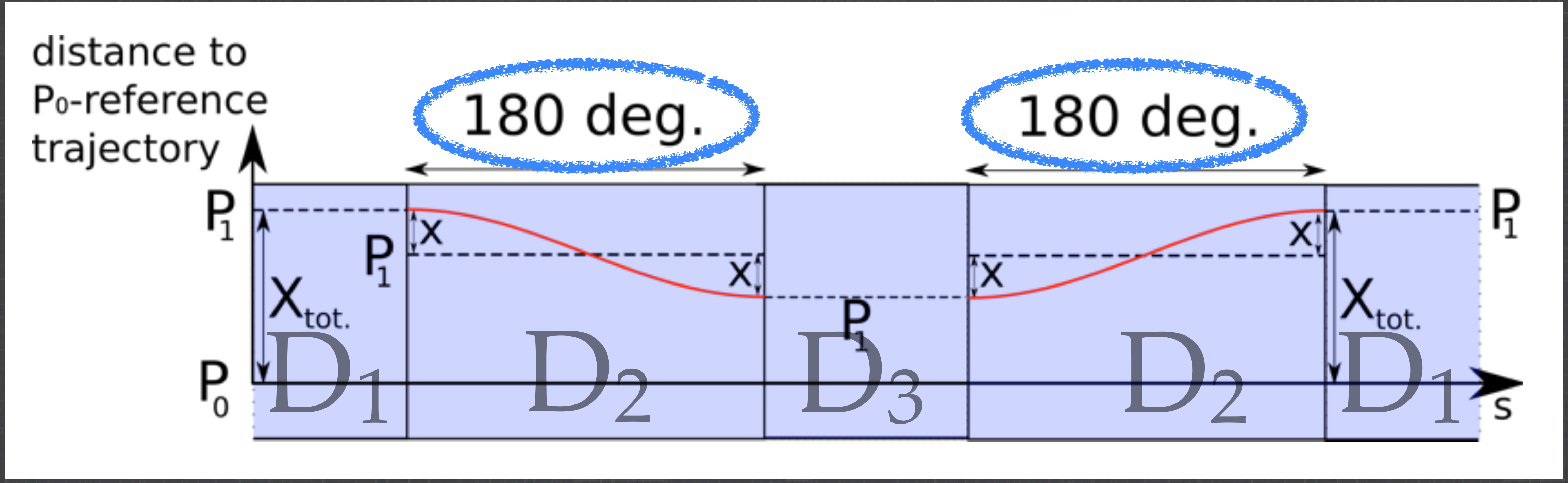

Insertions

Dispersion suppressor principle

Can be partial (lower picture) or complete (upper picture) dispersion suppression

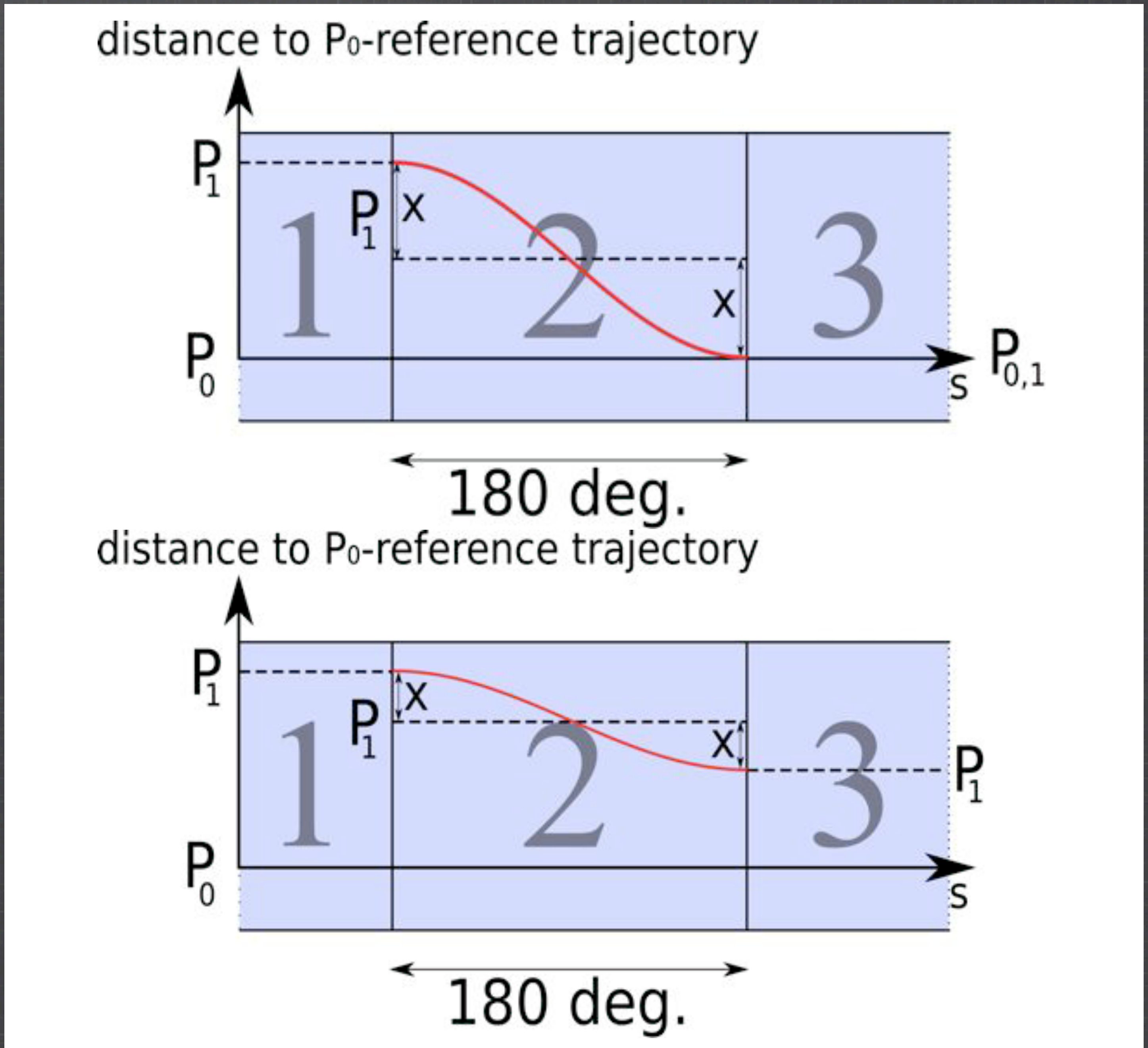

Insertions

Dispersion suppressor principle

Zero-chromatic system as long as amplitude detuning can be neglected.

→ several dispersion suppressors in cascade if the difference of dispersion is too large

$$D_{ini} + (-1)^{n+1} D_{fin} = 2 \sum_{i=1}^{n} (-1)^{i+1} D_i$$

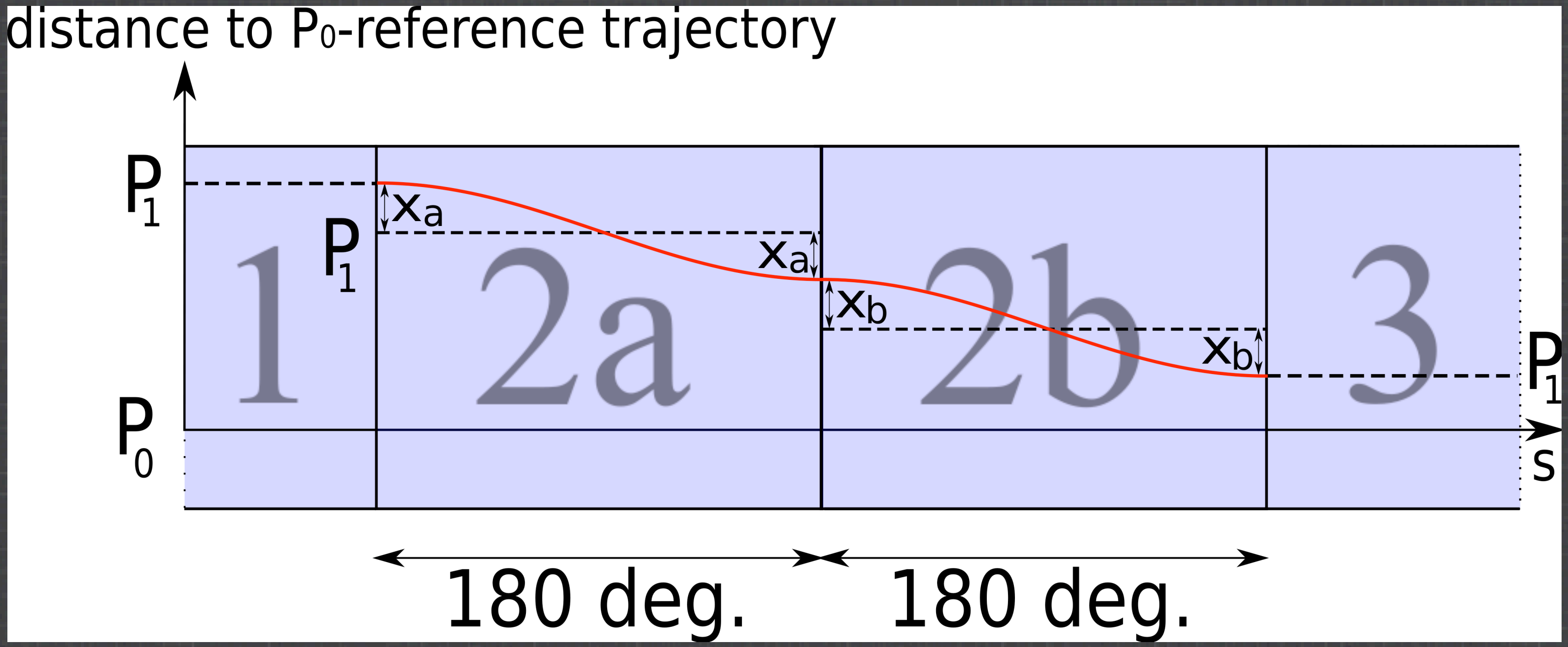

Outline

- Classic case: horizontal excursion circular FFAG
- Straight zero-chromatic FFAG
- FFAG insertions
- Vertical excursion FFAG
- Fixed frequency acceleration in zero-chromatic FFAGs

VERTICAL FFAG

Y. Mori

VERTICAL FFAG

- Proposed by Tihiro Ohkawa,
  (1955, JPS meeting, Phys. Rev. 110, 1247(1955))
  Rediscovered by S. Brooks.
  (2010, proc. of HB2010)
- Beam orbit rises vertically.
- Circumference is constant for all different beam energies.
- Accelerate relativistic (β~1) particles with fixed frequency RF field (Isochronous).
- Magnetic field configuration:
  - Increase exponentially in the vertical direction.
- Zero-chromaticity : Betatron tunes are always constant.
- **Electron cyclotron!**

G8. FFAG Electron Cyclotron.* TIHIRO OHKAWA, *University of Illinois*† (introduced by D. W. Kerst).—New types of FFAG[1] accelerators having the same orbit length for all momenta are proposed. In these types electrons, injected with an energy of a few Mev, are accelerated by a fixed frequency electric field until the radiation loss becomes serious, probably at a few Bev. The necessary cavity voltage is, for example, 200 Kev with 3 Mev injection energy. Two types of guiding fields, similar to Mark I (alternate field type) and Mark V (spirally ridged type) are used. In both, the magnetic field increases exponentially in the vertical direction so that as the particle energy increases, its orbit rises vertically. The field also depends on the radius and the azimuthal angle in such a way that the focusing properties are very similar, respectively, to Mark I and to Mark V. Other types of FFAG having the orbit surface not on a median plane are also proposed.

* Reported by the present author at the meeting of the Physical Society of Japan in June, 1955.
† On leave from the University of Tokyo.
[1] Reported by the present author at the meeting of the Physical Society of Japan in October, 1953; K. R. Symon Phys. Rev. 98, 1152(A) (1955).

Beam rises vertically.

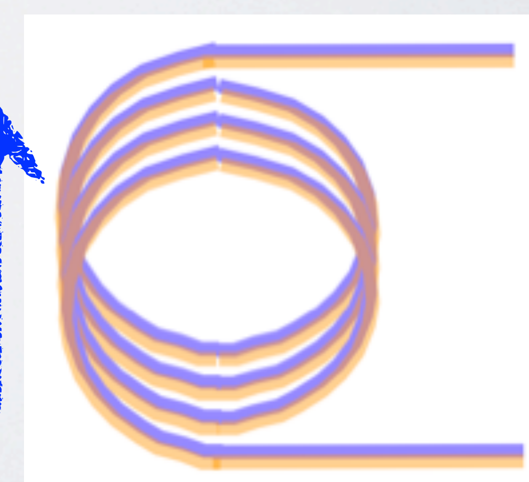

BETATRON MOTION

- Horizontal: $$\frac{d^2x}{d\theta^2} + \left[\frac{eB_y}{p}R - 1\right]R = 0$$
- Vertical: $$\frac{d^2y}{d\theta^2} + \frac{eB_x}{p}R^2 = 0$$
- Magnetic field: linearization

$$B_y = B_0 + \underline{\frac{\partial B_y}{\partial x}}x + \underline{\frac{\partial B_y}{\partial y}}y$$

$$B_x = \underline{\frac{\partial B_x}{\partial x}}x + \underline{\frac{\partial B_x}{\partial y}}y$$

Normal
Skew

- Orbit excursion
  - Vertical FFAG → Skew fields
- Betatron equations
  - x-y coupled

$$\frac{d^2x}{d\theta^2} + x + \frac{\rho}{B_0}\left(\frac{\partial B_y}{\partial y}\right)y = 0$$

$$\frac{d^2y}{d\theta^2} - \frac{\rho}{B_0}\left(\frac{\partial B_x}{\partial x}\right)x = 0$$

ZERO-CHROMATICITY

- Magnetic field $B_0 \approx B_y,\ div\ \vec{B} = 0 \rightarrow \dfrac{\partial B_x}{\partial x} = -\dfrac{\partial B_y}{\partial y}$

- Betatron equations
$$\frac{d^2x}{d\theta^2} + x + \frac{\rho}{B_y}\left(\frac{\partial B_y}{\partial y}\right) y = 0,$$
$$\frac{d^2y}{d\theta^2} + \frac{\rho}{B_y}\left(\frac{\partial B_y}{\partial y}\right) x = 0.$$

- Chromaticity is zero, if
$$\begin{cases} \rho = \text{const.}, \\ \dfrac{\rho}{B_y}\left(\dfrac{\partial B_y}{\partial y}\right) = l = \text{const.} \end{cases}$$

$$\longrightarrow \boxed{B_y = B_y^0 \exp\left(\frac{l}{\rho} y\right)}$$

MAGNETIC FIELD FOR ZERO-CHROMATICITY

- **Ring** (equations with $s = R\Theta = \rho\theta$)
  - H-FFAG
    $$\begin{cases} \dfrac{R}{\rho} = \text{const.}, \\ \dfrac{R}{B_y}\left(\dfrac{\partial B_y}{\partial x}\right) = k = \text{const.} \end{cases} \longrightarrow \boxed{B_y = B_y^0 \left(\dfrac{R}{R_0}\right)^k}$$
  - V-FFAG
    $$\begin{cases} \rho = \text{const.}, \\ \dfrac{\rho}{B_y}\left(\dfrac{\partial B_y}{\partial y}\right) = l = \text{const.} \end{cases} \longrightarrow \boxed{B_y = B_y^0 \exp\left(\dfrac{l}{\rho} y\right)}$$
- **Straight line**
  - H-FFAG
    $$\begin{cases} \rho = \text{const.}, \\ \dfrac{\rho}{B_y}\left(\dfrac{\partial B_y}{\partial x}\right) = n = \text{const.} \end{cases} \longrightarrow \boxed{B_y = B_y^0 \exp\left(\dfrac{n}{\rho} x\right)}$$
  - V-FFAG
    $$\begin{cases} \rho = \text{const.}, \\ \dfrac{\rho}{B_y}\left(\dfrac{\partial B_y}{\partial y}\right) = l = \text{const.} \end{cases} \longrightarrow \boxed{B_y = B_y^0 \exp\left(\dfrac{l}{\rho} y\right)}$$

ZERO-CHROMATIC MAGNETIC FIELD

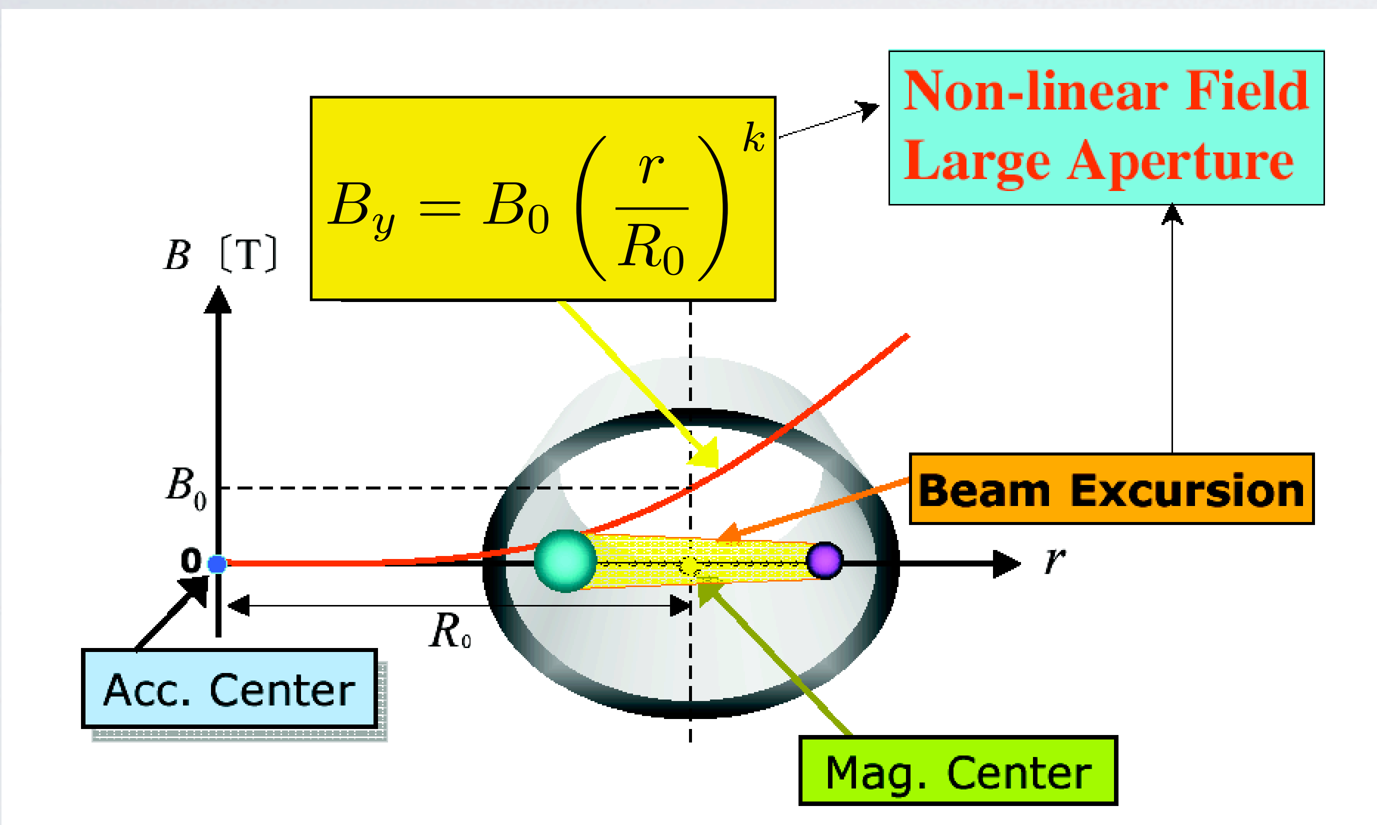

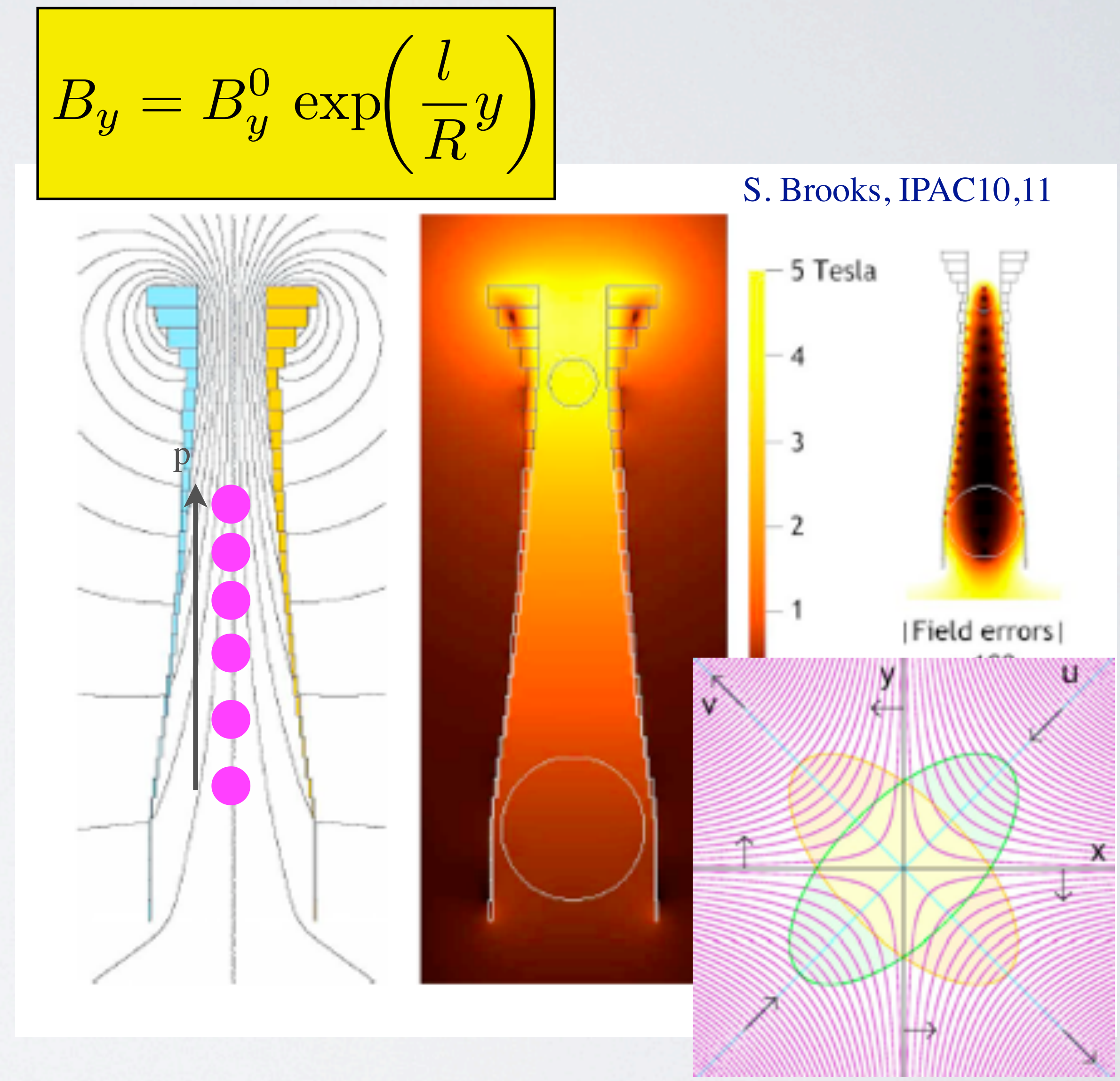

H-FFAG

V-FFAG

Outline

- Classic case: horizontal excursion circular FFAG
- Straight zero-chromatic FFAG
- FFAG insertions
- Vertical excursion FFAG
- Fixed frequency acceleration in zero-chromatic FFAGs

Fixed frequency acceleration

- Harmonic number jump acceleration

  T. Planche *et al*, “Harmonic number jump acceleration of muon beams in zero-chromatic FFAG rings”, Nucl. Instr. Meth. A, vol. 632, pp. 7–17, 2011.

- Serpentine acceleration

  E. Yamakawa *et al*, “Serpentine acceleration in zero-chromatic FFAG accelerators”, Nucl. Instr. Meth. A, vol. 716, pp. 46–53, 2013.

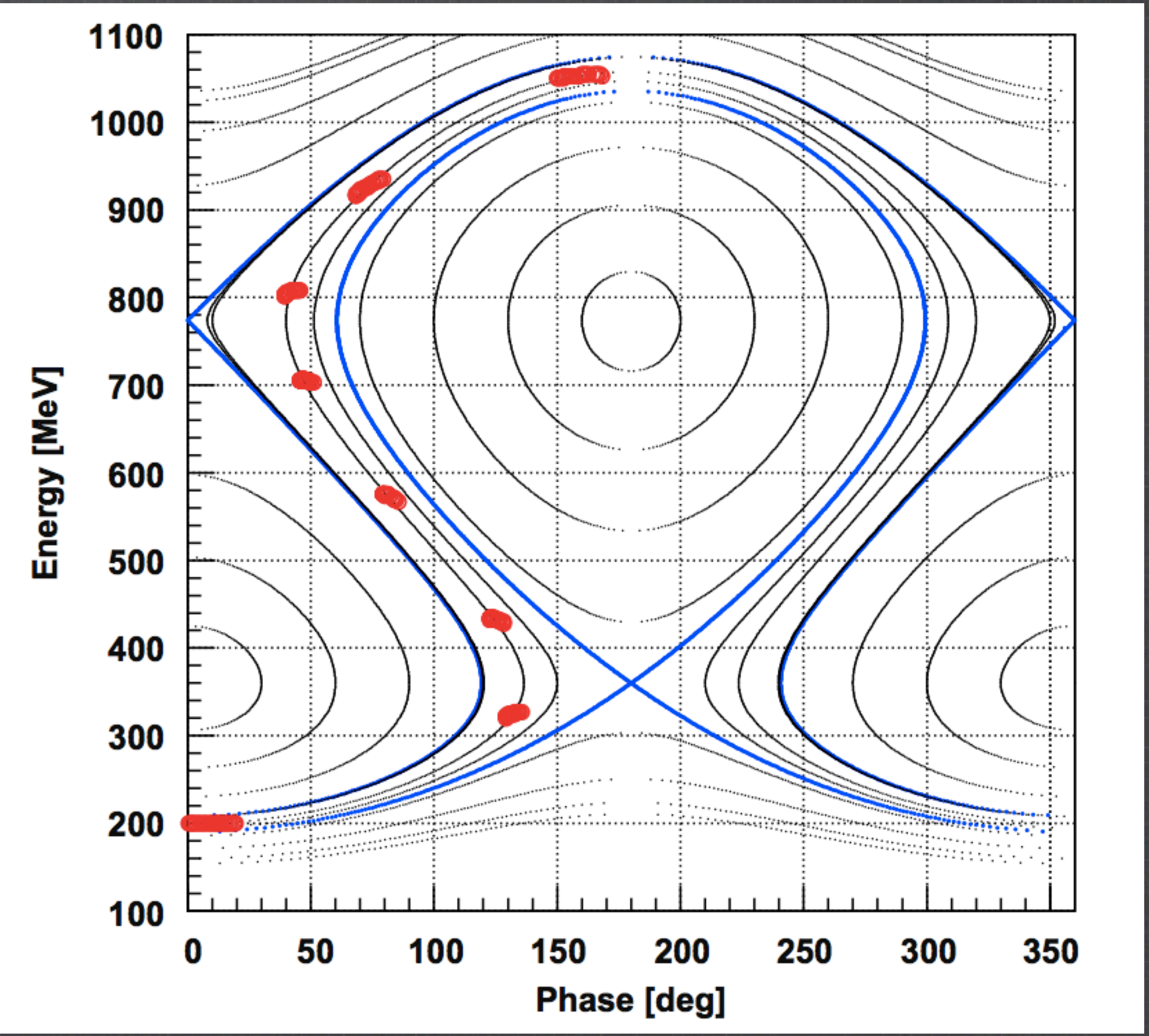

Summary

- Exponential field law fo zero-chromatic straight FFAG.
- Field law clarified experimentally.
- Combination of FFAG cells with matching of cell dispersion and matching of betafunctions.
- Dispersion suppressor to match cells with different dispersions.
- Vertical excursion FFAG to accelerate relativistic particles with fixed RF frequency.
- Fixed frequency acceleration schemes in zero-chromatic FFAGs.

Conclusion

- Strong revival of FFAGs in the last decade.
- Different ring shapes now possible.
- Insertions can be developped in FFAG rings.
- Isochronous rings for ultra-relativistic particles with vertical FFAG.

This is just the beginning!

Thank you for your attention

β_1 measurement

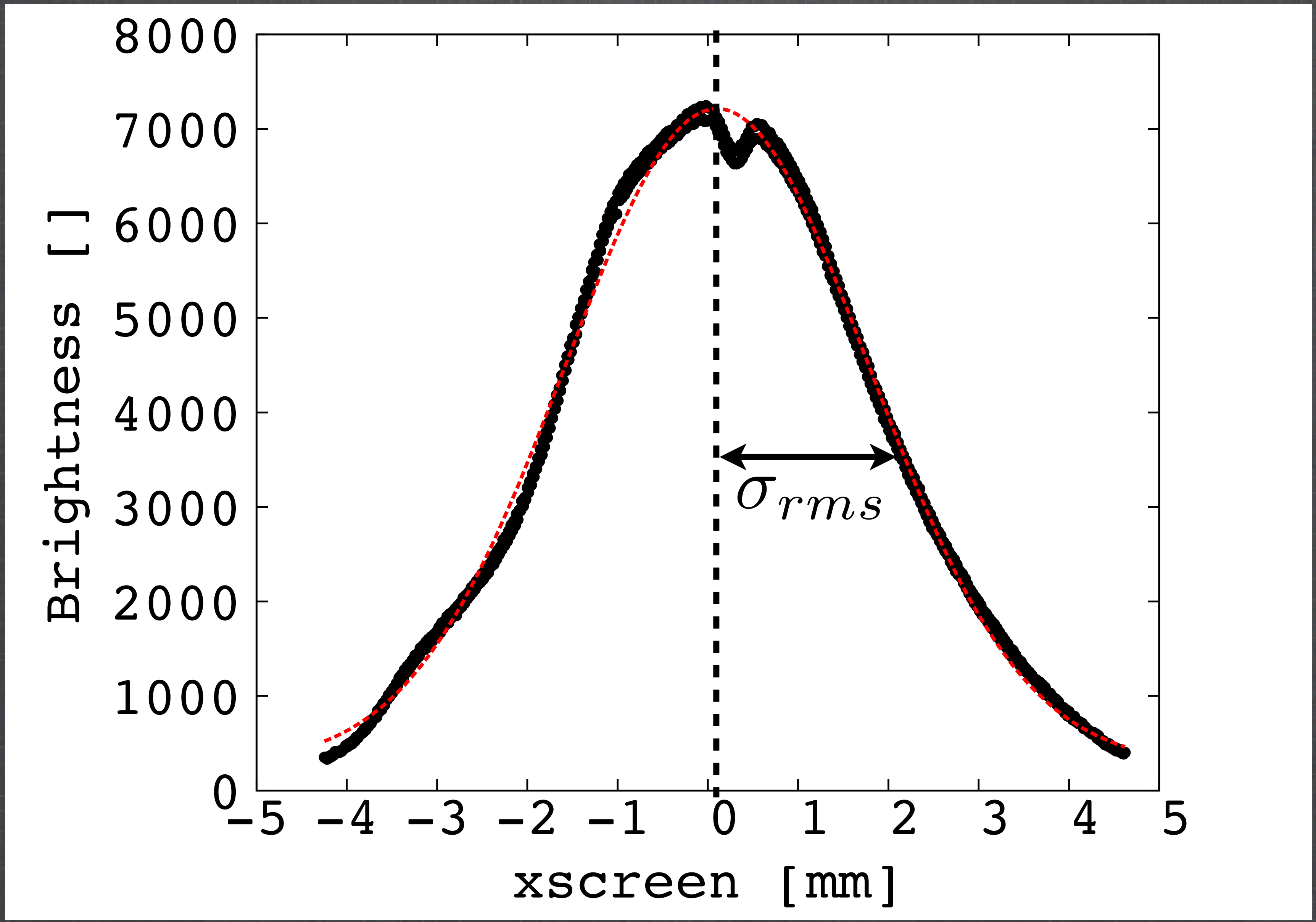

$$\beta_1 = \frac{\sigma_{rms}^2}{\epsilon_{rms}}$$

α_1 measurement

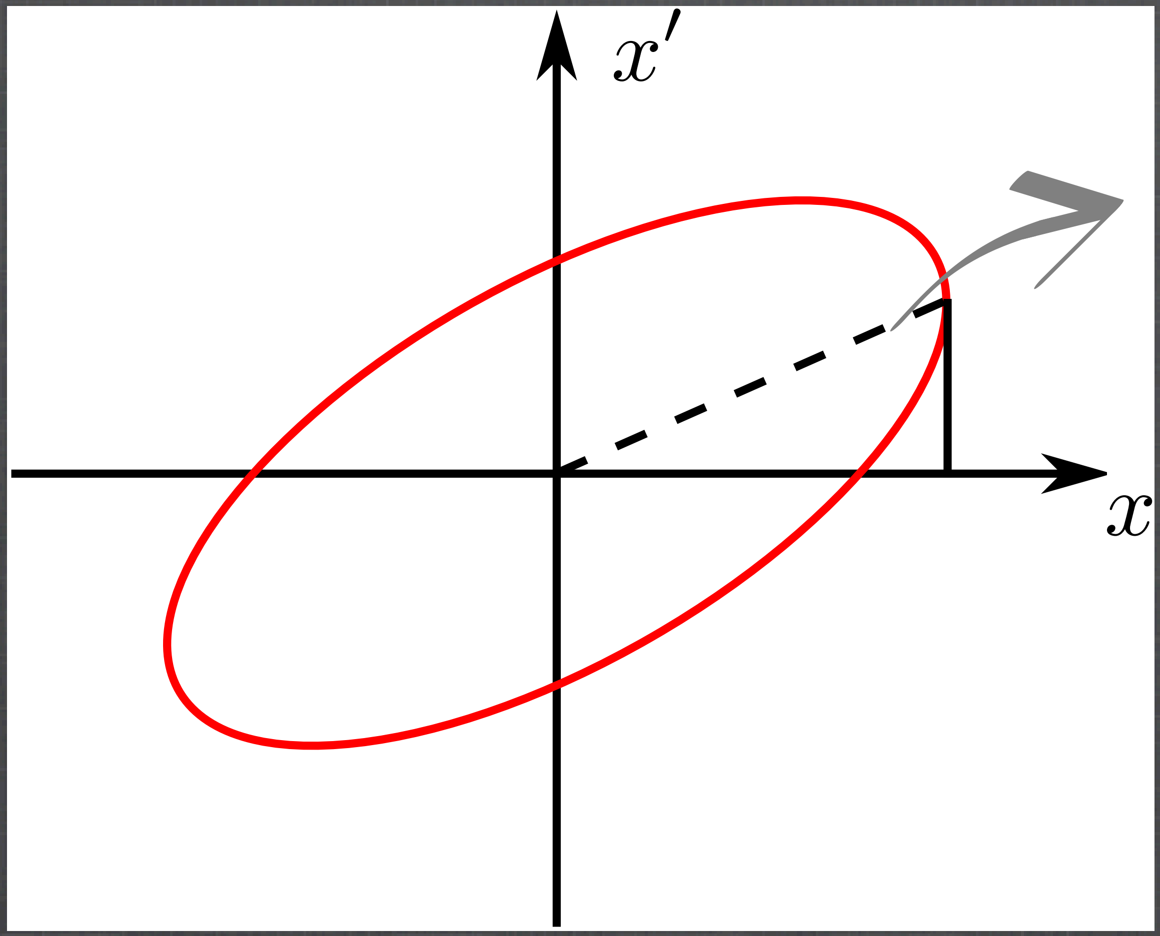

$$slope = -\left(\frac{\alpha}{\beta}\right)_{slit}$$

$$\alpha_1 = \beta_{slit}\left(\frac{\alpha}{\beta}\right)_{slit} - L\left(\frac{1}{\beta_{slit}} + \beta_{slit}\left(\frac{\alpha}{\beta}\right)_{slit}^2\right)$$

$$\beta_{slit} = \frac{\beta_1 + \sqrt{\beta_1^2 - 4L^2\left(1 - 2L\left(\frac{\alpha}{\beta}\right)_{slit} + L^2\left(\frac{\alpha}{\beta}\right)_{slit}^2\right)}}{2\left(1 - 2L\left(\frac{\alpha}{\beta}\right)_{slit} + L^2\left(\frac{\alpha}{\beta}\right)_{slit}^2\right)}$$

Experimental results

	x_1 (mm)	x'_1 (mrad)	σ (mm)	$\left(\frac{\alpha}{\beta}\right)_{slit}$ (m^{-1})
Ref. traj. 11 MeV	0.1	-0.5	1.7	-0.09
+10 mm 11 MeV	1.4	-1.8	1.6	-0.08
-10 mm 11 MeV	-2.6	2.9	1.4	-0.11
Ref. traj. 7 MeV	0.6	0.5	1.1	-0.09
+10 mm 7 MeV	0.3	-1.9	1.1	-0.05
-10 mm 7 MeV	-3.4	2.2	1.8	-0.11

Error estimation

Dominated by the beta error due to the fluctuation of the beam size.

statistical and independent error from the variation of rms beam size σ_{rms}.

error for 11 MeV: 3.7%

error for 7 MeV: 11.1%